EurJOC European Journal of Organic Chemistry

FULL PAPER

DOI: 10.1002/ejoc.201402634

Synthesis of *trans*-A_2B_2- and *trans*-A_2BC-Porphyrins with Polar 4′-(Dimethylamino)tolan-4-yl Substituents, and a Screening Protocol for Vapor-Phase Deposition on Metal Surfaces

Mariza N. Alberti,[a] Sylwia Nowakowska,[b] Manolis D. Tzirakis,[a] Jan Nowakowski,[c] Petra Fesser,[a] W. Bernd Schweizer,[a] Aneliia Shchyrba,[b] Carlo Thilgen,[a] Thomas A. Jung,*[b,c] and François Diederich*[a]

Keywords: Supramolecular chemistry / Self-assembly / Surface analysis / Dipole effects / Gold / Porphyrinoids

The role of polar 4-[*p*-(dimethylamino)phenylethynyl]phenyl substituents, with a calculated dipole moment of 3.35 Debye, in the self-assembly of *trans*-A_2B_2- and A_2BC-substituted porphyrins was explored in the solid state by X-ray crystallography, and on an Au(111) surface by scanning tunneling microscopy (STM). Our results demonstrate that the dipolar character of these substituents blocks the 2D self-assembly of porphyrins into larger ordered domains on Au(111) at low coverage, whereas antiparallel dipole–dipole interactions govern the molecular ordering in the crystal. The STM analysis revealed an adaptation of the conformation of the prochiral building blocks and a site-selectivity of the adsorption. We present a general protocol for testing the suitability of higher-molecular-weight compounds, such as porphyrins, to be deposited on surface by sublimation in ultra-high vacuum (UHV). This protocol combines classical methods of chemical analysis with typical surface science techniques.

Introduction

Supramolecular chemistry gives the opportunity to direct the self-assembly of molecular architectures using a variety of binding motifs or synthons that, depending on their relative association strengths, also give rise to subtle modifications of the resulting structures. In view of the rapidly growing number of well-defined supramolecular architectures[1,2] that can be constructed and investigated for potential uses, for example, in electronics[3] or medicine,[4] there is great demand for newly synthesized, shape-persistent π-conjugated molecules bearing various specific functional groups. Importantly, there are fundamental differences between the supramolecular architectures produced from solution by crystallization and those created at solid/liquid or solid/vacuum interfaces. Structural analysis of these architectures provides insight into the forces and interactions that lead to self-assembly in the different environments.

[a] Laboratorium für Organische Chemie, ETH Zurich, Vladimir-Prelog-Weg 3, 8093 Zurich, Switzerland
E-mail: diederich@org.chem.ethz.ch
http://www.diederich.ethz.ch/
[b] Institute of Physics, University of Basel, Klingelbergstrasse 82, 4056 Basel, Switzerland
E-mail: thomas.jung@psi.ch
https://nanolab.unibas.ch/
[c] Laboratory for Micro- and Nanotechnology, Paul Scherrer Institute, 5232 Villingen, Switzerland
E-mail: thomas.jung@psi.ch

Supporting information for this article is available on the WWW under http://dx.doi.org/10.1002/ejoc.201402634.

Given the planarity and stability of many porphyrins, on-surface assembly of porphyrin-based materials is of special interest.[5] A variety of *meso* substituents have been used to induce the formation of specific arrangements through noncovalent[6] or covalent[7] interactions. In some cases, porphyrin-based systems showed complex multiphase behavior due to the presence of different competing interactions.[8] In this regard, the on-surface self-assembly of a porphyrin bearing a polar 4′-(dimethylamino)tolan-4-yl (DMAT) *meso* substituent (cf. **1**, Figure 1; tolane = diphenylacetylene) has recently been explored.[9,10] Specifically, the polarity of this group, with a computed[11] dipole moment along the molecular axis of 3.35 Debye (see Section 5 in the Supporting Information), led to a complex interplay of attractive and repulsive, short- and long-range forces that allowed the dimensionality of on-surface assemblies to be controlled.[9]

In an extension of our studies, we were interested in further examining the role of the DMAT substituent in the solid state and in 2D supramolecular architectures. For this purpose, a systematic series of *trans*-A_2B_2 and *trans*-A_2BC porphyrins **1**–**6** (Figure 1) with different *meso* substituents was synthesized. The self-assembling behavior of these porphyrins in the solid state (porphyrins **1**, **2**, **4**, and **6**) and on a metallic surface (porphyrins **2** and **6**) was then investigated. A key step in the preparation of porphyrins **1**–**6** was the Suzuki–Miyaura cross-coupling of a porphyrinbis(boronic ester) with the appropriate aryl halides. When $[Pd(PPh_3)_4]$ was used as a catalyst in this reaction, two

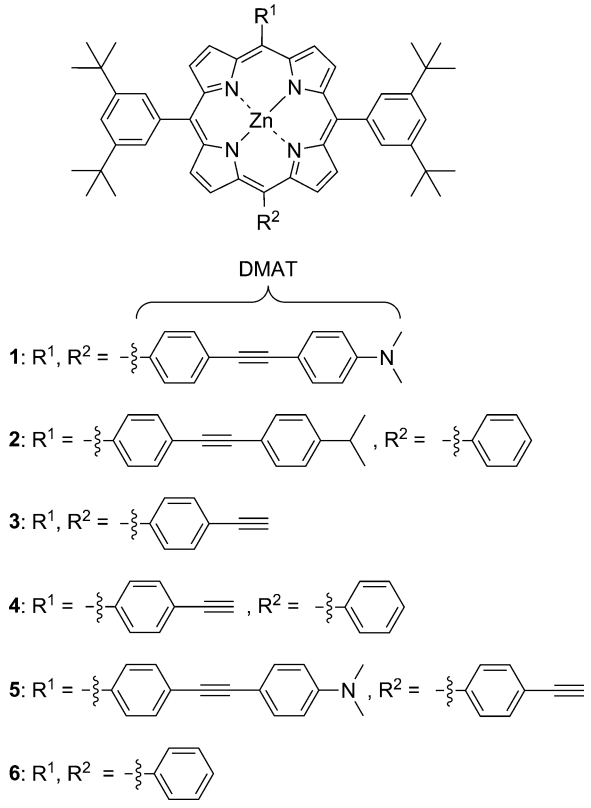

Figure 1. *trans*-A_2B_2 and *trans*-A_2BC porphyrins investigated in this study.

meso-phenylated porphyrins were formed as by-products. It is worth mentioning that, in comparison to our previous studies,[9,10] the modification of the molecular architectures described in this paper led, in some cases, to larger porphyrins with higher molecular weights. The larger the compounds are, the higher the temperature required for their sublimation, and, therefore, the more likely their fragmentation during the deposition process. In order to ensure that our investigations were performed on supramolecular assemblies formed from intact molecular modules, we developed a systematic screening protocol for the candidate molecules consisting of (i) sublimation in a test chamber under high vacuum (HV)[12] followed by high-performance liquid chromatography (HPLC), gel-permeation chromatography (GPC), NMR spectroscopy, high-resolution mass spectrometry (HRMS), and, optionally, thermogravimetric analysis (TGA) of the sublimed compound; (ii) electron spectroscopy for chemical analysis (ESCA)/X-ray photoelectron spectroscopy (XPS); and (iii) scanning probe microscopy (SPM) imaging.

Results and Discussion

Synthesis of Porphyrins 1–6

Although *trans*-A_2B_2 porphyrins can, in principle, be obtained by mixed condensation of pyrrole and two different aldehydes (A-CHO and B-CHO), this method is practically limited since it gives a statistical mixture of six different porphyrins (types A_4, A_3B, *cis*-A_2B_2, *trans*-A_2B_2, AB_3, and B_4). A selective way to obtain *trans*-A_2B_2 systems involves the MacDonald-type [2+2] condensation of a dipyrromethane with an aldehyde.[13] Self-condensation of dipyrromethane-1-carbinols or 1-acyldipyrromethane has also been used for the synthesis of porphyrins with this *meso* substitution pattern.[14] Another common route to both *trans*-A_2B_2 and *trans*-A_2BC systems uses a stepwise approach where *meso*-disubstituted *trans*-A_2-porphyrins are subjected to further *meso* functionalization.[15] In this case, *trans*-A_2-porphyrins can simply be synthesized by MacDonald-type [2+2] condensation of unsubstituted dipyrromethane with an aldehyde A-CHO.

For the preparation of target porphyrins **1**–**6** (Figure 1), we chose a stepwise approach to prevent scrambling of the *meso* substituents. An initially synthesized *trans*-A_2-porphyrin was metalated and then further *meso*-functionalized (see Section 2.1 in the Supporting Information). Using this method, porphyrin-bis(boronic ester) **7**[16] (Scheme 1), the common precursor of all of the target porphyrins (i.e., **1**–**6**), was prepared in four steps and 10% overall yield (see Scheme S2 in the Supporting Information).

In the key step of the synthesis, a Suzuki–Miyaura cross-coupling of bis(boronic ester) **7** with aryl bromide **8** was used to obtain porphyrin **1** (Scheme 1). Compound **8** was prepared in 92% yield by Sonogashira cross-coupling of 1-bromo-4-iodobenzene with 4-ethynyl-*N*,*N*-dimethylaniline (see Section 2.2 in the Supporting Information). Unexpectedly, the Suzuki–Miyaura cross-coupling of **7** with **8** in the presence of [$Pd(PPh_3)_4$] as a catalyst (Route A, Scheme 1) gave a mixture of two porphyrins with molecular masses of 1186.56 Da (major product) and 1043.49 Da (minor product). Although attempts to fully separate these compounds by flash column chromatography (FC) were unsuccessful, we were able to isolate them by preparative recycling GPC (2× Jaigel-2H and Jaigel-2.5H, $CHCl_3$).[17] Gratifyingly, pure porphyrins **1** and **2** (Scheme 1) could be fully characterized by NMR spectroscopy and MALDI-TOF mass spectrometry. Importantly, an unambiguous assignment was possible by ^{13}C NMR spectroscopy. In the spectrum of D_{2h}-symmetric *trans*-A_2B_2 derivative **1**, two resonances for both the α- and β-carbon atoms of the pyrrole rings are expected, and they were observed at δ = 150.04 and 150.64 ppm (C-α), and at δ = 133.00 and 134.45 ppm (C-β). In contrast, C_{2v}-symmetric *trans*-A_2BC derivative **2** showed four C-α resonances at δ = 150.04, 150.26, 150.61, and 150.65 ppm, and four C-β resonances at δ = 132.43, 132.56, 132.98, and 134.46 ppm.

To explain the origin of by-product **2**, we considered two routes through which **2** could be formed. These involve either a further transformation of **1** or the transfer of a phenyl group from the catalyst [$Pd(PPh_3)_4$] to porphyrin **7**.[18,19] To test the first possibility, we studied the stability of porphyrin **1** under the conditions of synthetic Route A (Scheme 1). The lack of any transformation clearly indicates that **2** is not generated via **1**. With the hope of proving the

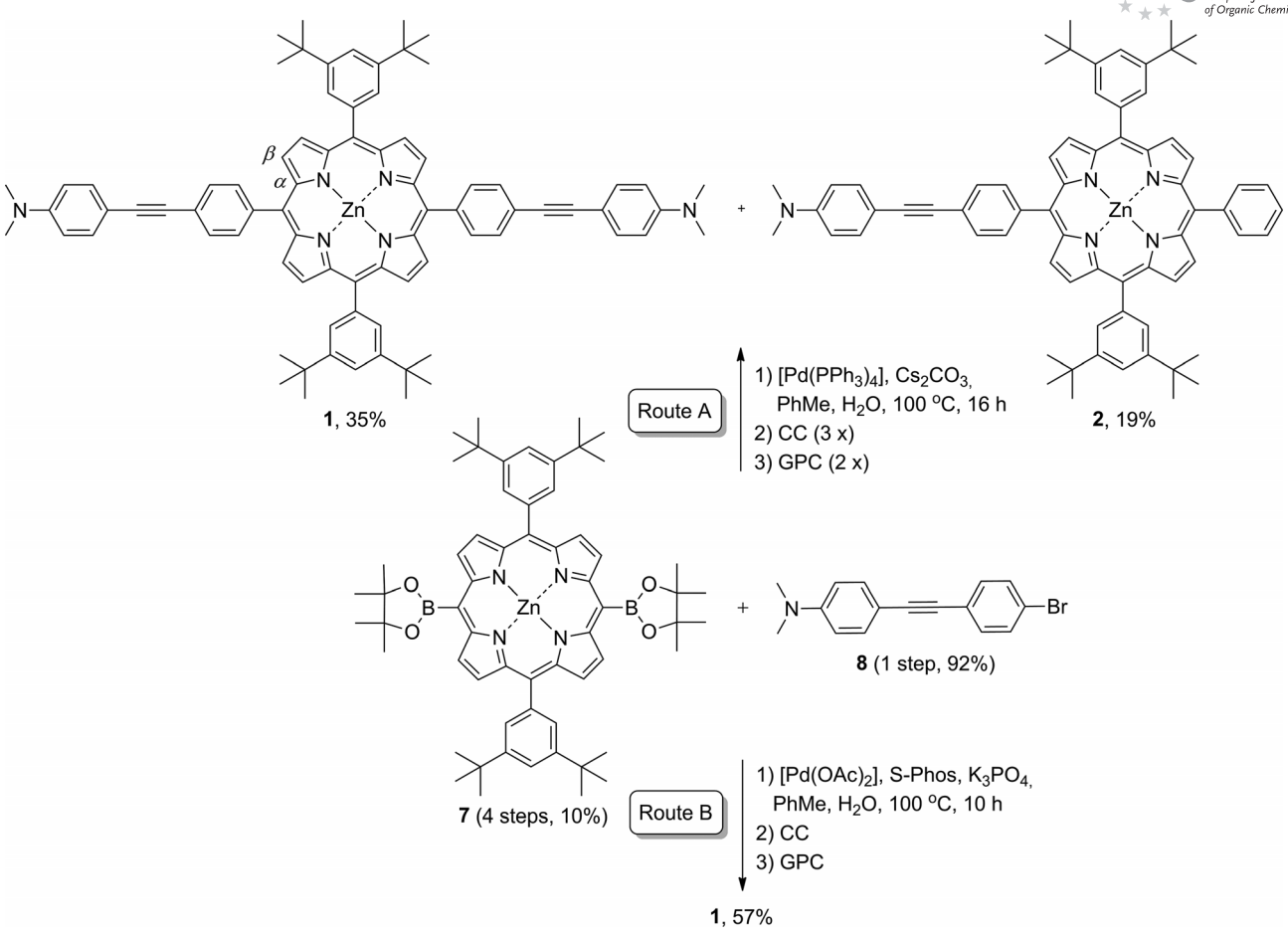

Scheme 1. Synthesis of porphyrins **1** and **2**.

validity of our second hypothesis, we carried out the Suzuki–Miyaura cross-coupling of **7** with **8** in the presence of $[Pd(OAc)_2]$ and the bulky phosphine ligand dicyclohexyl-2-(2,6-dimethoxyphenyl)phenylphosphine (S-Phos; Route B, Scheme 1).[20] In this case, porphyrin **1** was exclusively formed in 57% yield. This observation undoubtedly supports the proposal that by-product **2** is formed by phenyl–aryl exchange during the cross-coupling reaction (aryl = DMAT). A plausible mechanism for this exchange is presented in Scheme 2.[18] Specifically, the first step of the catalytic cycle consists of the oxidative addition of bromide **8** to Pd^0 to form Pd^{II} complex **9**. As an "irregular" step of this mechanism, an exchange between a phosphorus-bound phenyl ligand and the palladium-bound aryl group (R^1) originating from **8** occurs to give complex **10**. Reaction of the latter with Cs_2CO_3 leads to an exchange of bromide with carbonate to form **11**, which, by transmetalation with boronate **12**, gives complex **13**. In the final reductive elimination step, the phenyl ligand of Pd^{II} complex **13** is now coupled (instead of the desired aryl residue R^1) to the porphyrin core to give the scrambled porphyrin (i.e., **2**) and regenerate the palladium catalyst.

With diacetylene-appended porphyrin **1** in hand, we set out to study its [2+2] cycloaddition–retroelectrocyclization (CA–RE) reaction[21] with different electron-deficient olefins. Specifically, the reaction of porphyrin **1** with 7,7,8,8-tetracyano-*p*-quinodimethane (TCNQ; 2.1 equiv.) was quantitative and regioselective, giving product **14**[22] (Scheme 3, a). To further expand the scope of the CA–RE on-surface reaction,[10] we initially examined the possible regular [AB]-polymerization of porphyrin **1** (A) with doubly reactive bis(dicyanovinyl) arene **15** (B; 1.2–5 equiv.) in 1,1,2,2-tetrachloroethane (Scheme 3, b). This reaction was monitored by MALDI-TOF mass spectrometry. The reaction of **15** with a similar substrate incorporating two reactive 4-ethynylanilino sites (i.e., 1,4-bis{[4-(*N*,*N*-dihexylamino)phenyl]ethynyl}) had previously been demonstrated to give oligomeric and macrocyclic $[AB]_n$, $A[AB]_n$ as well as $B[AB]_n$ structures.[23] In our reaction, the consumption of porphyrin **1** and the formation of a mixture of oligomeric products were observed. The signals seen in the mass spectrum of the crude product correspond to *m*/*z* values that are consistent with products of three general formulae, i.e., $[AB]_n$ (n = 1 or 2), A[AB], and $B[AB]_n$ (n = 1 or 2; A and B denote the two monomers **1** and **15**, respectively). B[AB]-type push–pull chromophore **16** was the major product, and was isolated in 64% overall yield (consistently with previous findings, this product was formed in

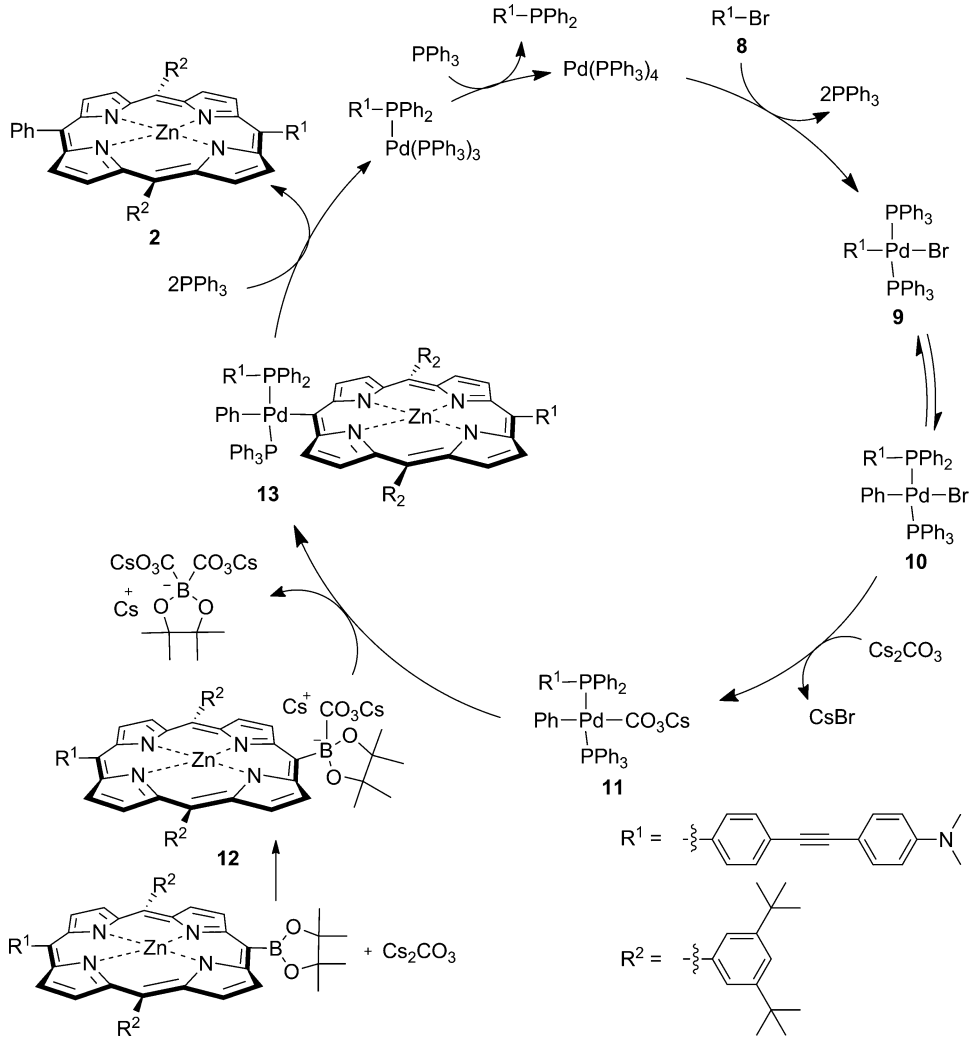

Scheme 2. Proposed catalytic cycle accounting for the unexpected formation of porphyrin **2**.[18]

a regioselective manner). The other products were formed in minor amounts (5–10%), and were only detected by MALDI-TOF mass spectrometry. At this point, we were interested in examining the reactivity of the two more accessible dicyanovinyl groups of **16**. Hence, the reaction of **16** with a 30-fold excess of porphyrin **1** was investigated in 1,1,2,2-tetrachloroethane at 120 °C. Under these conditions, the starting material was consumed, but only unidentified products were formed. Similar studies were also performed for porphyrin **2** (see Section 2.3 in the Supporting Information).

The synthesis of porphyrins **3**, **4**, and **6** was accomplished in a manner analogous to that described for **1** and **2** (Scheme 4). Suzuki–Miyaura cross-coupling of porphyrin **7** with bromide **17**, which was obtained in 79% yield according to a known literature procedure,[24] in the presence of $[Pd(PPh_3)_4]$ as a catalyst, gave porphyrins **18** and **19** in 69 and 21% yields, respectively. When the coupling reaction was carried out in the presence of $[Pd(OAc)_2]$ and S-Phos, porphyrin **18** was formed exclusively in 82% yield. It can be concluded that scrambled porphyrin **19** is formed analogously to **2** (cf. Scheme 2). In the next step, the *i*Pr_3Si protecting groups were removed from **18** and **19** with *n*Bu_4NF in THF to give porphyrins **3** and **4** in 68 and 79% yields, respectively. Similarly, porphyrin **6** was prepared in 88% yield by Suzuki–Miyaura cross-coupling of porphyrin **7** with iodobenzene (Scheme 4).

Porphyrin **5** was synthesized by Sonogashira cross-coupling of **3** with 4-bromo-*N*,*N*-dimethylaniline (1 equiv.; see Scheme S2 in the Supporting Information). The reaction conditions[25–27] screened for this transformation are summarized in Table S2. In particular, porphyrin **5** (11% yield) was formed only when $[Pd_2(dba)_3]$ (dba = dibenzylideneacetone) and P(*o*-Tol)$_3$ were used as the catalytic system (Table S2, entry 4). It is worth mentioning that GPC facilitated purification of the desired porphyrin; using this method, aromatic impurities could be removed smoothly.

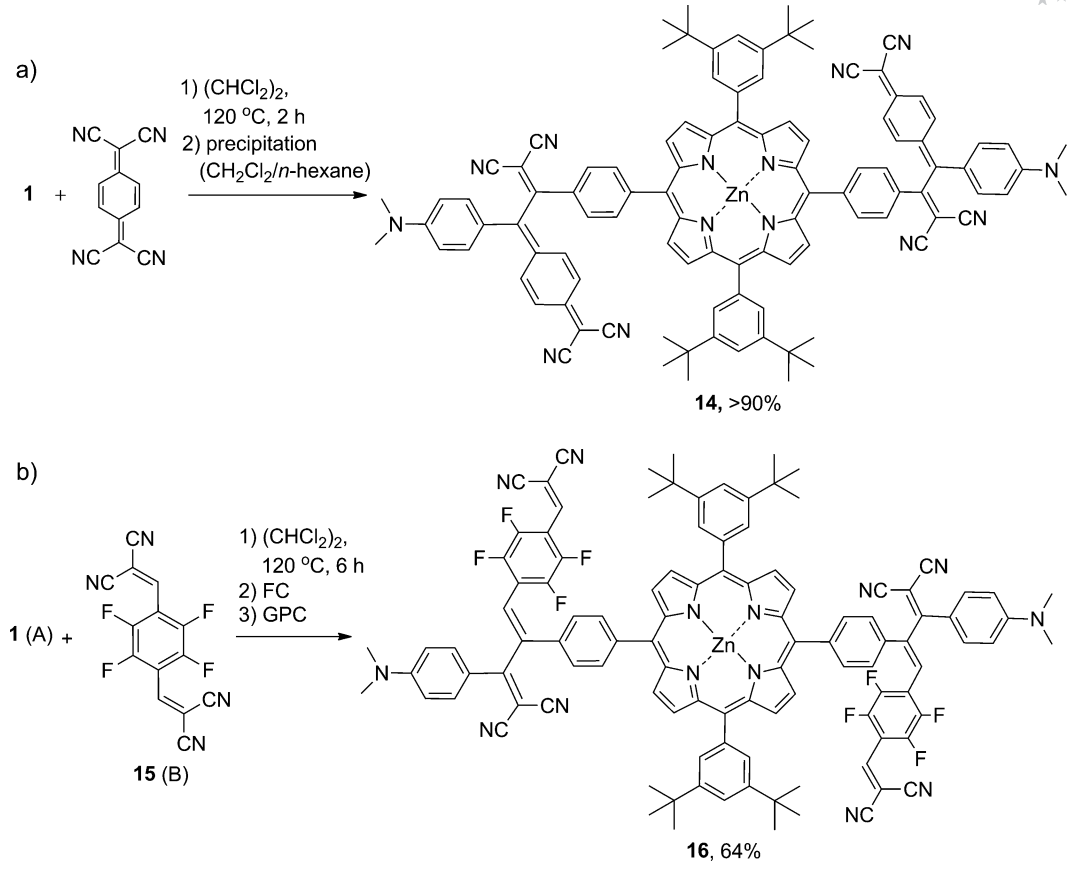

Scheme 3. CA–RE reaction of porphyrin **1** with a) TCNQ and b) bis(dicyanovinyl) arene **15**.

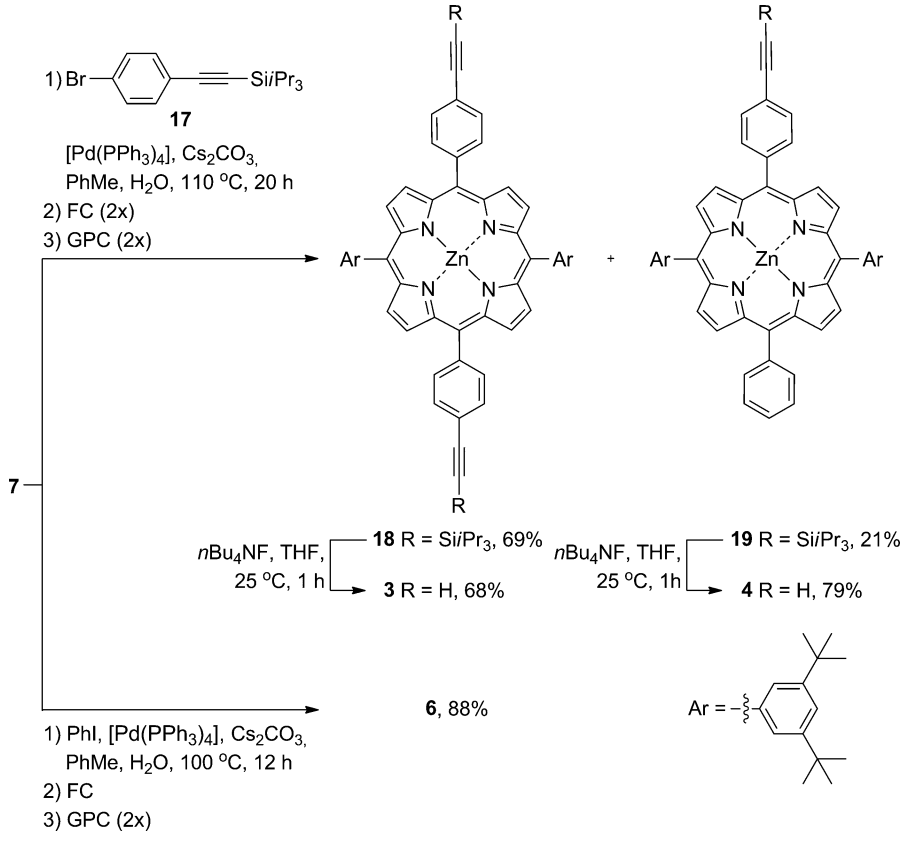

Scheme 4. Synthesis of porphyrins **3**, **4**, and **6**.

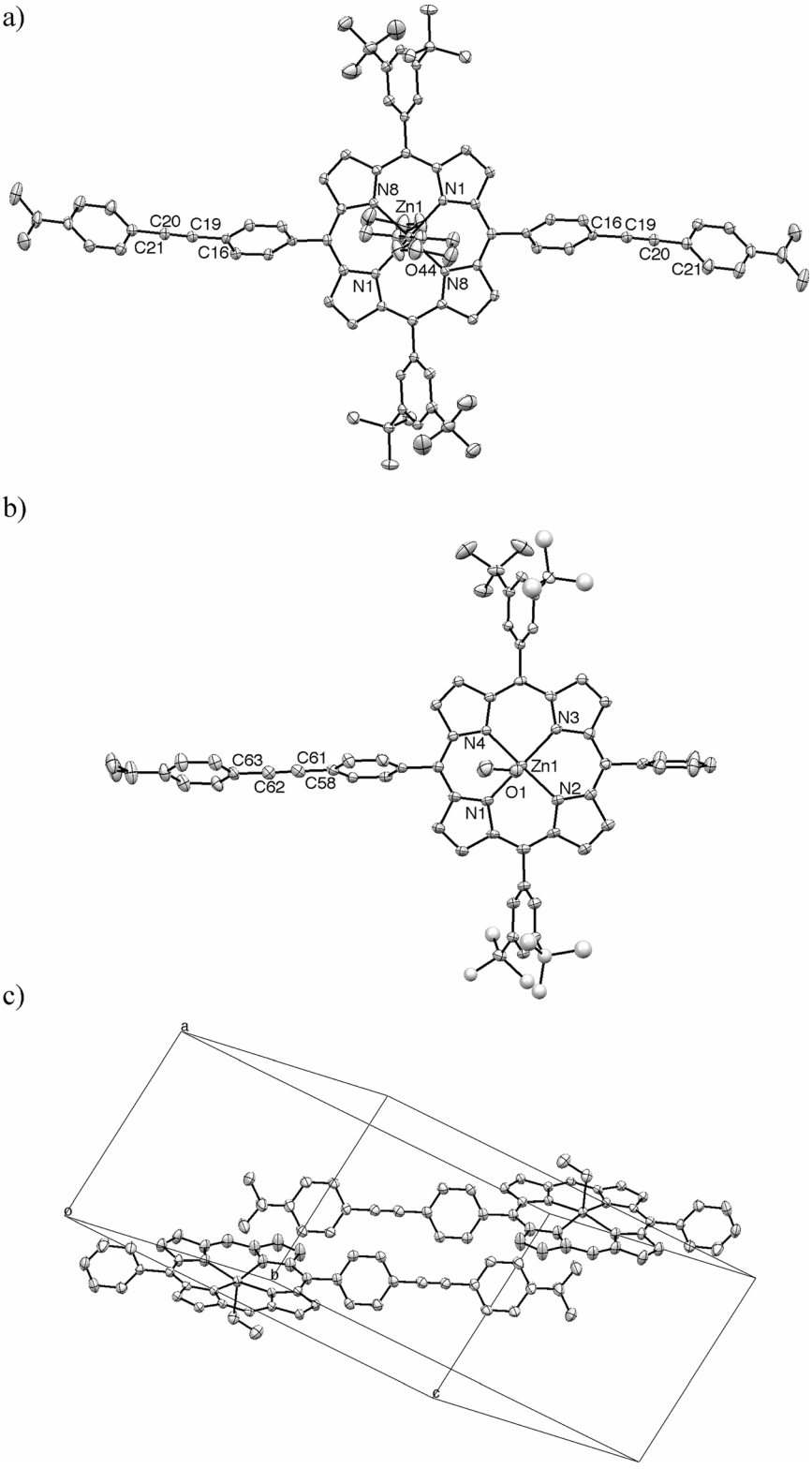

Figure 2. ORTEP plots of a) **1**·2THF and b) **2**·MeOH, with vibrational ellipsoids shown at the 50% probability level (T = 100 K). Arbitrary numbering. Noncoordinating solvent molecules, hydrogen atoms, and disordered positions are omitted for clarity. c) View of the unit cell of **2**·MeOH. 3,5-Di(*tert*-butyl)phenyl rings, noncoordinating solvent molecules, hydrogen atoms, and disordered positions are omitted for clarity. Selected bond lengths [Å] and angles [°]: **1**·2THF: Zn-1–N-1: 2.059(2), Zn-1–N-8: 2.046(2), Zn-1–O-44: 2.336(2), C-16–C-19: 1.443(3), C-19–C-20: 1.200(3), C-20–C-21: 1.437(3), N-1–Zn-1–N-1: 180.000(1), N-8–Zn-1–N-8: 180.00(6), N-1–Zn-1–O-44: 90.41(7), N-8–Zn-1–O-44: 89.93(7), O-44–Zn-1–O-44: 179.999(1), C-19–C-20–C-21: 178.9(3), C-20–C-19–C-16: 175.5(3); **2**·MeOH: Zn-1–N-1: 2.069(3), Zn-1–N-2: 2.064(3), Zn-1–N-3: 2.063(3), Zn-1–N-4: 2.063(3), Zn-1–O-1: 2.131(3), C-58–C-61: 1.423(5), C-61–C-62: 1.206(5), C-62–C-63: 1.444(5), N-3–Zn-1–N-1: 162.7(1), N-4–Zn-1–N-2: 164.5(1), N-1–Zn-1–O-1: 95.3(1), N-3–Zn-1–O-1: 102.0(1), C-62–C-61–C-58: 178.6(4), C-61–C-62–C-63: 177.8(4). Further details are found in Sections 4.2 and 4.3 of the Supporting Information.

X-ray Crystallography

X-ray crystal structures of porphyrins **1**, **2**, **4**, **6**, and **19** were solved. The structures of **1** and **2**, which have DMAT substituents, are discussed here, whereas all other structural information can be found in the Supporting Information. Single crystals of porphyrin **1** were obtained from a mixture of THF and CH_3CN (2:1) by slow evaporation at 3–5 °C. The compound (Figure 2, a) cocrystallizes with two THF molecules axially coordinated to the zinc(II) ion, and further gap-filling, disordered THF/CH_3CN molecules, in the centrosymmetric, triclinic space group $P\bar{1}$ with the octahedrally coordinated zinc(II) ion at the inversion point. The macrocycle is essentially planar with an average deviation from the 24-atom porphyrin plane of 0.03 Å. The O-atoms of the THF ligands lie on an axis, which is nearly perpendicular to the porphyrin plane. Both Zn–O bond lengths are 2.336(2) Å, which is in the expected range for porphyrins with axial oxygen-containing ligands.[28,29] The dihedral angles between the porphyrin plane and the *meso* aryl rings are 72° and 62°, respectively. The phenyl rings interconnected by an acetylene unit are twisted by 74° relative to each other.

Single crystals of porphyrin **2** were obtained from a mixture of CH_2Cl_2 and MeOH (2:1) by slow evaporation at 3–5 °C. The structure of **2**·MeOH (triclinic space group $P\bar{1}$, Figure 2, b) shows an almost planar porphyrin core with an average deviation from the 24-atom porphyrin plane of 0.04 Å. The zinc(II) ion prefers a square-pyramidal coordination geometry, and is axially coordinated by a MeOH ligand. Similar to other pentacoordinate metalloporphyrin structures, the zinc(II) ion deviates from the mean plane of the four pyrrolic N-atoms towards the axial MeOH ligand by 0.295 Å. The dihedral angles between the porphyrin plane and the *meso* aryl rings vary between 63° and 86°. The perpendicular arrangement of the 4-(dimethylamino)-phenyl substituent between two porphyrin rings related by a translation along the *b*-axis causes big gaps between the molecules, which are filled with a mixture of heavily disordered methanol and dichloromethane molecules. Each 4-(dimethylamino)phenyl ring is in close proximity to the porphyrin ring of an adjacent molecule (Figure 2, c), participating in one C–H···N[30] and two C–H···π[31] interactions (for selected interactions and geometrical parameters, see also Figure S6 and Table S5 in the Supporting Information).

Porphyrin **2** has a substantial permanent electric dipole moment of 3.72 Debye (calculated value,[11] see Section 5 in the Supporting Information), which is induced across the molecule by its *N*,*N*-dimethylanilino (DMA) moiety. This dipole moment gives rise to electrostatic interactions, which lead to an antiparallel dipolar alignment of the two porphyrins in the unit cell. Consistently with this observation, porphyrin **2** undergoes analogous self-assembly in solution, as suggested by the characteristic upfield shifts of the $N(CH_3)_2$, 9-H, and 10-H protons that are seen in the ^{1}H NMR spectrum ($CDCl_3$) when the concentration is increased (carbon atom numbering and ^{1}H NMR spectra are shown in Figure S2 in the Supporting Information). Of course, we were interested in exploring whether this distinct antiparallel dipolar alignment of porphyrin **2** would also be found in 2D self-assembly on metal surfaces.

A Three-Step Protocol for Determining the Suitability of Molecular Modules for Deposition on Surfaces by Sublimation in Ultra-High Vacuum

A comparison between the solid-state ordering induced by the DMAT moiety in the synthesized porphyrins and 2D self-assemblies formed on the chemically inert and atomically clean Au(111) surface under UHV (ultra-high vacuum) conditions is possible only if the molecular modules can be assembled at the solid/vacuum interface in the absence of impurities and decomposition products. Although deposition by sublimation is well established, it has been reported that for some molecules, thermal decomposition takes place before or during sublimation.[32] In addition, decomposition may occur rapidly after deposition on some metallic surfaces.[33] The fact that molecules can decompose during UHV deposition asks for a careful investigation of this process. As degradation may occur at different stages of the process (i.e., in the bulk of the heated material or at crystal surfaces), and considering the fact that SPM methods are quite time-consuming, a three-tiered approach (Figure 3) was developed to detect possible decomposition prior to microscopic investigations.

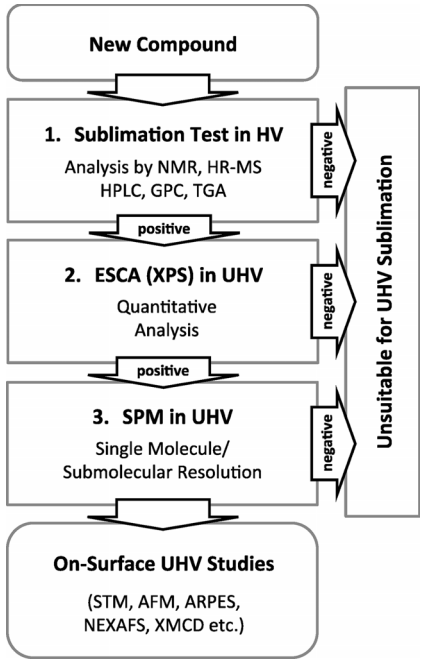

Figure 3. A general protocol for conveniently checking the intactness of molecules deposited on a surface by sublimation in UHV. Molecules passing the entire test are suitable for on-surface UHV studies by, among other methods, scanning tunneling microscopy (STM), atomic force microscopy (AFM), angle-resolved photoemission spectroscopy (ARPES), near edge X-ray absorption fine structure (NEXAFS), X-ray magnetic circular dichroism (XMCD).

In the first screening step, a specially built apparatus for sublimation under HV (high vacuum) conditions is used.[12] The compound to be tested (1–2 mg) is placed in a quartz flask, heated with a tin bath, and sublimed onto a cold finger. The sublimed material is washed from the cold finger, and analyzed by NMR spectroscopy, HRMS, HPLC, and/or GPC to assure that it is chemically intact. Ideally, the analysis of the sublimate would be complemented by an examination of the unsublimable residue. If these leftovers correspond to a considerable amount of decomposed/polymerized material, then such a thermal conversion may prevent successful deposition in UHV,[34] which is usually preceded by extended degassing procedures. In this case, thermogravimetric analysis (TGA) under the conditions of the degassing procedure is advisable (see Section 6 in the Supporting Information). The sublimation of impure compounds may also release a significant amount of contaminants. This is due to the temperature dependence of sublimation and the possibility of impurities being more volatile than the target compound. Therefore, all compounds are carefully purified by column chromatography, GPC, and/or HPLC before entering the first screening stage.

In the second screening step, the molecular material is introduced into a UHV chamber, properly degassed, and sublimed onto a sample surface with the rate being controlled by a quartz crystal microbalance (QCMB). Fluctuations in the deposition rate at a constant crucible temperature may be attributed to pressure bursts originating from undesired thermal gradients in the crucible and/or thermally activated chemical reactions. For this reason, the deposited sample is checked by ESCA (XPS) with a particular focus on its elemental composition. If the results deviate from the theoretical values, the experiment is repeated for a different molecular coverage to find out whether contaminations are present in the starting sample or whether a chemical reaction occurs during degassing, sublimation, or deposition.

However, it may also happen that the molecules decompose on the surface and the resulting fragments remain adsorbed. Such decomposition cannot be detected by ESCA, and neither can it be detected in the first screening step, since the cold finger is made of a different material (glass, quartz) from the substrate (metal), and relatively few of the sublimed molecules are in direct contact with it. Therefore, in the third and final screening step, the integrity of the material deposited at sub-ML[35] coverage on the desired surface is checked with an SPM technique that is able to resolve single molecules or even submolecular units.

Examining the Suitability of Porphyrins 1–6 for Deposition by Sublimation in UHV

Despite their high molecular weight and labile functional groups (absent in **6**), porphyrins **1**–**4** and **6** could be sublimed without fragmentation or decomposition at 10^{-6}–10^{-7} mbar and bath temperatures of 400–440, 320–340, 300–330, 290–320, and 270–310 °C, respectively, as con-

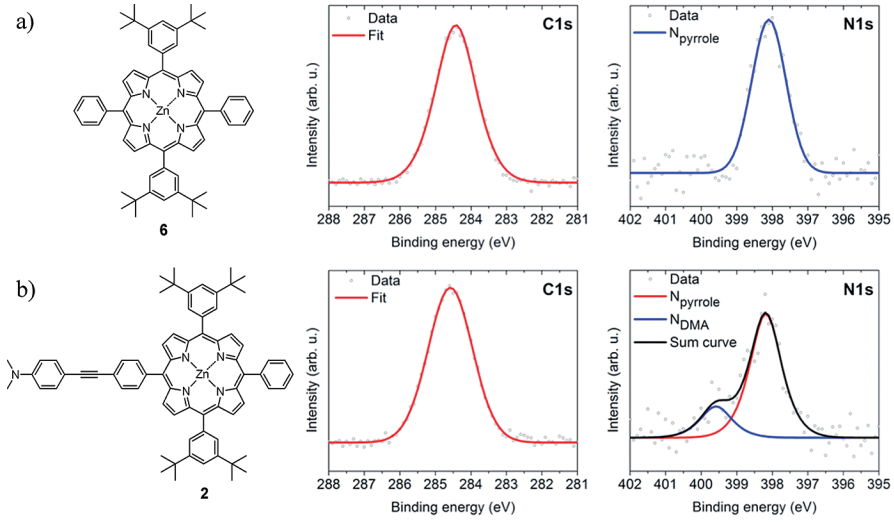

c)

Porphyrin	C/N		$N_{pyrrole}/N_{DMA}$	
	XPS	Theoretical	XPS	Theoretical
6	16.9	16.0	n/a	n/a
2	17.0	14.8	4	4

Figure 4. C1s and N1s XPS spectra of a multilayer of a) porphyrin **6** and b) porphyrin **2** on Au(111). c) Summary of the quantitative analysis comparing the experimental C/N and $N_{pyrrole}/N_{DMA}$ ratios with the theoretical values; n/a: not applicable.

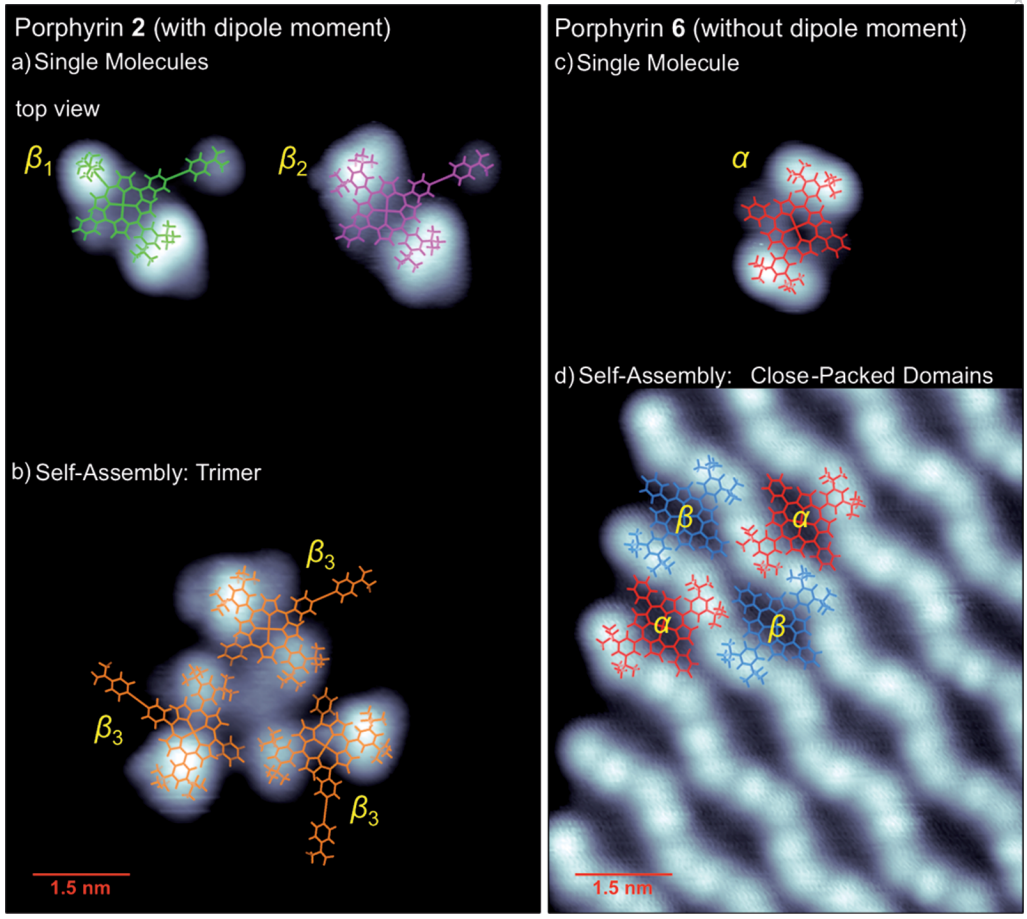

Figure 5. Role of the polar DMAT residue in on-surface self-assembly. a and b) STM images of β-enantiomers[36a] of polar porphyrin **2** deposited on Au(111): a) two different chiral conformers denoted β_1 and β_2; b) trimer consisting of identical chiral conformers denoted β_3. c and d) STM images of apolar porphyrin **6** deposited on Au(111): c) single α-enantiomer [α and β differ in the signs of the dihedral angles between the porphyrin core and each of the 3,5-di(*tert*-butyl)phenyl groups]; d) close-packed domain consisting of two enantiomeric conformers (α and β), arranged in alternating order. Tentative models are superimposed on the STM images. Removal of the polar substituent leads to a uniform condensation, which shows that the polarity of porphyrin **2** is blocking the self-assembly into ordered domains. All STM measurements were carried out at 5 K; tunneling parameters: a) 1.00 V/10 pA, b) 1.20 V/5 pA, c) 0.05 V/5 pA, and d) 0.20 V/10 pA.

firmed by the analytical techniques used in the first screening step (Figure 3). In contrast, porphyrin **5** decomposed during sublimation at 10^{-6}–10^{-7} mbar and bath temperatures of 370–420 °C, as shown by NMR spectroscopy and HRMS. Therefore, it was excluded from further studies.

For the second screening stage, porphyrins **1**–**4** and **6** were placed in a home-made stainless steel crucible and introduced into a UHV system with a base pressure of 5×10^{-11} mbar. Stable deposition rates were achieved only for porphyrins **2** and **6**, of which several monolayers were sublimed onto Au(111). The recorded XPS spectra are shown in parts a and b of Figure 4 (for general XPS conditions, see Section 1.4 in the Supporting Information). Porphyrin **6** bears four pyrrolic nitrogen atoms, which are characterized by a single peak at the binding energy (BE) of 398.1 eV. The N1s spectrum of porphyrin **2** has two components, one originating from the four pyrrolic nitrogen atoms (398.2 eV), and the other from the nitrogen atom of the DMA moiety (399.6 eV). All N1s BEs are in good agreement with the data published for a similar (*N*,*N*-dimethylanilino)ethynyl-substituted tetraarylporphyrin.[10] Furthermore, the quantitative analysis presented in Figure 4 (c) reveals a good agreement between the experimental (16.9) and the theoretical (16.0) C/N ratios for **6**. In the case of porphyrin **2**, the agreement between the C/N ratios is acceptable (experimental 17.0 vs. theoretical 14.8); the excess of carbon possibly results from incomplete degassing of the material in the crucible. Taking into account the perfect $N_{pyrrole}/N_{DMA}$ ratio, a repetition of the deposition for XPS measurements was not necessary. Although porphyrin **1** passed the first screening stage, its deposition onto Au(111) by sublimation under UHV conditions was problematic. A factor that needs to be taken into account is the higher molecular mass of **1** (1186.56 Da) compared to porphyrins **2**–**6** (900.41–1067.48 Da). Remarkably, successful STM studies on a *trans*-A_2B_2 porphyrin lighter by only 84 Da,[26,36] show that, in addition to the molecular mass, also the chemical nature of the residues {i.e., two *meso*-[4-

(4-pyridyl)ethynyl]phenyl[26,36] vs. two *meso*-DMAT (in **1**) substituents} strongly influences the stability of the porphyrins during sublimation.

Porphyrins **3**–**5**, which did not pass the second screening step, bear either one or two 4-ethynylphenyl *meso* substituents. Previous studies have shown that a diethynyl-substituted π-system polymerizes on Ag(111), Au(111), and Cu(111) after annealing at ca. 125 °C,[37] a temperature which is much lower than the sublimation temperature of **3**–**5** (290–420 °C). This brings us to the conclusion that the sublimation rate of ethynylated porphyrins steadily decreases over time because of competitive polymerization processes such as Glaser coupling[38] in the crucible. This is consistent with the observed degradation of porphyrins **3**–**5** upon prolonged heating at high temperatures (200–250 °C).

Last but not least, the STM images of single molecules of porphyrins **2** and **6** (vide infra; Figure 5, a and c) are in good agreement with their molecular structures and, consequently, these molecules successfully passed the whole screening test.

On-Surface (2D) Self-Assembly: STM Investigations

Among the six porphyrins **1**–**6** synthesized in this study, only **2** and **6** successfully passed the whole screening test (Figure 3), and could thus be further used for on-surface studies. At this point, it is important to point out that porphyrin **6** has no net dipole moment due to its *trans*-A_2B_2 substitution pattern with two 3,5-di(*tert*-butyl)phenyl and two phenyl substituents. In contrast, the DMA moiety of *trans*-A_2BC-porphyrin **2** induces a permanent electric dipole moment across the molecule (calculated to be 3.72 Debye; see Section 5 in the Supporting Information).

Detailed STM studies were performed at 5 K on Au(111) with a coverage of ca. 0.2 ML of **2**. Individual molecules can be identified (Figure 5, a; tunneling parameters 1.00 V/10 pA) by their characteristic signature, which manifests itself in the conformation-dependent STM contrast of the 3,5-di(*tert*-butyl)phenyl and DMA groups in conjunction with the contrast of the porphyrin macrocycle. The characteristic contrast of different subunits appears even more clearly in the STM image of porphyrin **6** (Figure 5, c; tunneling parameters 0.05 V/5 pA). The different levels of STM contrast observed for the 3,5-di(*tert*-butyl)phenyl groups depend on the dihedral angle between this group and the porphyrin core, and they can be used to analyze the conformation of the molecule, including its conformational chirality, as established in earlier studies.[9,10,36,39] If the torsion angles around the bonds interconnecting the porphyrin and the 3,5-di(*tert*-butyl)phenyl rings are negative (a viewer looking along an interannular bond can make the ring planes eclipse by anticlockwise rotation of the proximal ring through less than 90°), the conformational enantiomer is termed "α"; if the torsion angles are positive, the enantiomer is termed "β".[36a] Although conformers of both chirality senses, "α" and "β", can be observed for porphyrin **2** on the surface, only β is shown in Figure 5 (a), as chirality is not in the focus of the current study. The β_1 and β_2 conformers (Figure 5, a) differ in the absolute value of the dihedral angles between the porphyrin core and each of the 3,5-di(*tert*-butyl)phenyl groups. The DMA group of both conformers appears with a dimmer contrast than the 3,5-di(*tert*-butyl)phenyl groups.[9,10] The supramolecular trimers, shown in Figure 5 (b) (tunneling parameters 1.20 V/5 pA), consist of identical conformational enantiomers (β_3) which, similar to β_1 and β_2, show specific torsional angles between the porphyrin core and each of the 3,5-di(*tert*-butyl)phenyl groups. In any case, these dihedral angles are smaller than those observed in the X-ray crystal structure of **2**. The porphyrins in these trimers are arranged "back-to-back", probably due to van der Waals interactions between the *tert*-butyl groups and C–H···π interactions between the *tert*-butyl and the phenyl groups, while the polar DMA groups stick out, which possibly stabilizes the porphyrin trimer against condensation to form higher oligomers. Similar self-assembly behavior was observed with a related A_3B-porphyrin on Au(111).[10] That A_3B-porphyrin was found to self-assemble in "open" (head-to-head) dimers, whereas no dimers were observed with **2**. This clearly shows that even a small modification in the structure of a porphyrin can lead to noticeable changes in its self-assembly behavior.

In contrast to **2**, porphyrin **6** does not include a polar group, which significantly changes the way it organizes on the surface. As seen in Figure 5 (d) (tunneling parameters 0.20 V/10 pA), it forms close-packed assemblies with alternating conformational enantiomers (α and β) held together by van der Waals interactions between the *tert*-butyl groups, and C–H···π interactions between the *tert*-butyl and the phenyl groups, similarly to the trimers of porphyrin **2**. This behavior further confirms that the DMA tail of **2** is blocking its self-assembly into larger oligomers or extended islands. In neither case (**2** or **6**) is the herringbone reconstruction, which is characteristic for Au(111),[40] influenced. As is often the case for heteroepitaxy on Au(111), the single molecules of both porphyrins, the trimers and the higher order islands of porphyrin **2** are adsorbed preferentially in the elbows of the reconstruction on the electronically poor fcc region. Furthermore, the edges of the self-assembled close-packed domain created from porphyrin **6** are straight (see Figure S1 in the Supporting Information), and the domain boundary is always located at the end of the fcc (face-centred cubic) region. This means that both porphyrins adsorb in a site-selective manner. Moreover, the facts that (i) the trimer is composed of identical conformers of porphyrin **2**, and (ii) the close-packed islands are made up of conformers of opposite chirality sense, arranged in a chessboard pattern, demonstrate the conformational adaptability of both porphyrins.

Although the polar DMAT tails led to isolated trimers on the Au(111) surface, their favorable antiparallel dipolar alignment enforced a close-packed arrangement of the molecules in the crystal (Figure 2, c). This shows that the assembly in 3D, as seen in the crystal structure, does not necessarily predict the 2D assembly on metal surfaces, which

is also influenced by the intrinsic properties of the surface and its interaction with the molecular modules.

Conclusions

A series of *meso*-substituted *trans*-A_2B_2 and *trans*-A_2BC poprhyrins **1**–**6** was synthesized in order to systematically study the role of the polar DMAT substituent in the 3D self-assembly of crystals and in the 2D supramolecular architectures formed on metal surfaces. The key step in their preparation was the Suzuki–Miyaura cross-coupling of a porphyrin-derived diboronate with the appropriate aryl halides in the presence of $[Pd(PPh_3)_4]$. Interestingly, porphyrins **2** and **4** were unexpectedly formed by transfer of a phenyl group from the PPh_3 ligand of the palladium catalyst to the metal and subsequent coupling to the porphyrin core.

The molecular structures and crystal packings of porphyrins **1**, **2**, **4**, **6**, and **19** were determined by X-ray crystallography. In all cases, the porphyrin core was found to be almost planar, and the zinc(II) ion preferred to be tetra-, penta-, or hexacoordinate with cocrystallized solvent molecules acting as axial ligands. The intermolecular interactions in crystalline porphyrin **2** – which shows a permanent dipole moment of 3.72 Debye, mainly originating from the DMAT substituent – are dominated by antiparallel dipole–dipole interactions.

A general protocol for testing the suitability of new compounds for deposition by sublimation under UHV conditions was developed and applied to porphyrins **1**–**6**. In particular, it became apparent that porphyrins having 4-ethynylphenyl groups with terminal acetylenes at the *meso* positions decompose upon prolonged heating. Also, the deposition by UHV sublimation of porphyrin **1**, which has the highest molecular mass (1186.56 Da) in the series, was problematic. These results underline the importance of having a convenient preselection procedure to identify worthwhile candidate molecules, thus avoiding time-consuming acquisition of inconclusive SPM data by imaging structures that have been modified during the deposition. We are convinced that this efficient screening protocol with its decent throughput will stimulate the development of molecular architectures suitable for SPM investigations.

STM studies of porphyrins **2** and **6** – which successfully passed the screening protocol – on Au(111) showed that the polar DMAT tail blocks the 2D self-organization into higher order oligomers or extended islands at low coverage. This contrasts with the 3D self-organization in a single crystal, where the antiparallel arrangement of the polar tails is the governing force of ordering. Moreover, the investigation of both porphyrins provided a deeper insight into the on-surface conformational adaptation of molecules and their site-selective adsorption.

Experimental Section

General Remarks: The procedures for the synthesis of **1**–**6**, **18**, and **19** are described below. Bromide **17** was prepared according to literature procedures.[24] The carbon-atom numbering is defined in the structures of compounds **1**–**6**, **18**, and **19** shown in the NMR section of the Supporting Information (Figures S28, S33, S38, S40, S42, S44, S59, and S61, respectively). The matrix used for MALDI MS was *trans*-2-[3-(4-*tert*-butylphenyl)-2-methyl-2-propenylidene]-malononitrile (DCTB).

[5,15-Bis[3,5-di(*tert*-butyl)phenyl]-10,20-bis(4-{2-[4-(dimethylamino)phenyl]ethynyl}phenyl)porphyrinato(2–)-κN^{21},κN^{22},κN^{23},κN^{24}]-zinc(II) (1) and [5,15-Bis[3,5-di(*tert*-butyl)phenyl]-10-(4-{2-[4-(dimethylamino)phenyl]ethynyl}phenyl)-20-phenylporphyrinato(2–)-κN^{21},κN^{22},κN^{23},κN^{24}]zinc(II) (2): A round-bottomed flask (100 mL) was evacuated and purged with N_2 (3×). Porphyrin **7** (500 mg, 0.50 mmol), $[Pd(PPh_3)_4]$ (58 mg, 0.05 mmol), and Cs_2CO_3 (2.12 g, 6.51 mmol) were added. The flask was carefully evacuated and purged with N_2 (3×). Bromide **8** (374 mg, 1.25 mmol), toluene (50 mL), and H_2O (200 μL) were added. The mixture was degassed by three freeze–pump–thaw cycles and put under N_2. It was heated to 100 °C for 16 h, and cooled to 25 °C. SiO_2 (ca. 15 g) was added, and the solvent was evaporated. Flash chromatography in the dark (3× SiO_2; *n*-pentane→CH_2Cl_2, 1% v/v Et_3N), followed by GPC (2× Jaigel-2H and Jaigel-2.5 H, $CHCl_3$), gave **1** (208 mg, 35%) and **2** (99 mg, 19%) as purple solids.

Data for porphyrin **1**: R_f = 0.06 (SiO_2; *n*-pentane/CH_2Cl_2, 2:1), m.p. > 300 °C. ^{1}H NMR (600 MHz, $CDCl_3$): δ = 1.53 (s, 36 H, *t*Bu), 3.02 (s, 12 H, Me), 6.73 (d, J = 8.4 Hz, 4 H, 8-H), 7.56 (d, J = 9.0 Hz, 4 H, 7-H), 7.80 (t, J = 1.8 Hz, 2 H, 4-H), 7.89 (d, J = 7.8 Hz, 4 H, 6-H), 8.09 (d, J = 1.8 Hz, 4 H, 3-H), 8.19 (d, J = 7.8 Hz, 4 H, 5-H), 8.97 (d, J = 4.8 Hz, 4 H, 1-H or 2-H), 9.01 (d, J = 4.8 Hz, 4 H, 1-H or 2-H) ppm. ^{13}C NMR (150 MHz, $CDCl_3$): δ = 31.89, 35.19, 40.43, 87.65, 91.77, 110.29, 112.10, 120.53, 120.99, 122.80, 123.44, 129.61, 129.83, 131.82, 132.57, 133.00, 134.45, 141.83, 142.36, 148.70, 150.04, 150.32, 150.64 ppm. IR (neat): $\tilde{\nu}$ = 2959 (m), 2901 (m), 2866 (m), 2796 (m), 2210 (m), 1807 (w), 1727 (w), 1697 (w), 1609 (m), 1592 (m), 1519 (m), 1491 (m), 1475 (m), 1442 (m), 1423 (w), 1391 (w), 1361 (m), 1337 (m), 1286 (m), 1246 (m), 1219 (m), 1196 (m), 1133 (m), 1101 (w), 1069 (m), 996 (s), 928 (m), 899 (w), 886 (w), 875 (w), 860 (m), 814 (s), 795 (s), 752 (w), 735 (w), 716 (s), 665 (w), 645(w) cm^{-1}. UV/Vis ($CHCl_3$): λ_{max} (ε, M^{-1}cm^{-1}) = 425 (680300), 550 (34535), 589(11500) nm. HRMS (MALDI, DCTB): *m*/*z* (%) = 1197.5604 (66), 1192.5596 (13), 1191.5571 (30), 1190.5555 (44), 1189.5577 (47), 1188.5574 (57), 1186.5570 (100); calcd. for $C_{80}H_{78}N_6{}^{64}Zn$ $[M]^+$ 1186.5574.

Data for porphyrin **2**: R_f = 0.06 (SiO_2; *n*-pentane/CH_2Cl_2, 2:1), m.p. > 300 °C. ^{1}H NMR (600 MHz, $CDCl_3$): δ = 1.53 (s, 36 H, *t*Bu), 2.99 (s, 6 H, Me), 6.71 (d, J = 8.4 Hz, 2 H, 10-H), 7.55 (d, J = 8.4 Hz, 2 H, 9-H), 7.73–7.77 (m, 3 H, 12-H and 13-H), 7.80 (br. s, 2 H, 6-H), 7.89 (d, J = 7.8 Hz, 2 H, 8-H), 8.10 (br. d, J = 1.2 Hz, 4 H, 5-H), 8.20 (d, J = 7.8 Hz, 2 H, 7-H), 8.23 (d, J = 6.6 Hz, 2 H, 11-H), 8.95 (d, J = 4.2 Hz, 2 H, 1-H, 2-H, 3-H or 4-H), 8.98 (d, J = 4.2 Hz, 2 H, 1-H, 2-H, 3-H or 4-H), 9.00 (d, J = 4.2 Hz, 2 H, 1-H, 2-H, 3-H or 4-H), 9.02 (d, J = 4.2 Hz, 2 H, 1-H, 2-H, 3-H or 4-H) ppm. ^{13}C NMR (150 MHz, $CDCl_3$): δ = 31.90, 35.19, 40.42, 87.65, 91.77, 110.32, 112.10, 120.45, 120.95, 121.16, 122.75, 123.44, 126.64, 127.58, 129.62, 129.88, 131.79, 131.98, 132.43, 132.56, 132.98, 134.46, 141.87, 142.38, 143.08, 148.70, 150.04, 150.26, 150.31, 150.61, 150.65 ppm. IR (neat): $\tilde{\nu}$ = 2958 (m), 2923 (m), 2854 (m), 2209 (w), 2158 (w), 1809 (w), 1700 (w), 1611 (w), 1591 (m), 1521 (m), 1487 (w), 1474 (m), 1459 (m), 1452 (m), 1425 (w), 1392 (w), 1361 (m), 1337 (m), 1287 (m), 1247 (m), 1214 (m), 1202 (m), 1154 (w), 1133 (m), 1102 (w), 1068 (m), 999 (s), 929 (m), 900 (m), 886 (w), 875 (w), 860 (w), 821 (m), 812 (m), 796 (s), 752 (s), 715 (s), 701 (s), 665 (m) cm^{-1}. UV/Vis ($CHCl_3$): λ_{max} (ε, M^{-1}cm^{-1}) =

423 (702400), 549 (31800), 589 (9200) nm. HRMS (MALDI, DCTB): *m*/*z* (%) = 1049.4852 (15), 1048.4827 (41), 1047.4808 (66), 1046.4832 (69), 1045.4818 (82), 1044.4866 (100), 1043.4833 (79); calcd. for $C_{70}H_{69}N_5{}^{64}Zn$ $[M]^+$ 1043.4844.

{5,15-Bis[3,5-di(*tert*-butyl)phenyl]-10,20-bis(4-ethynylphenyl)porphyrinato(2–)-κ*N*^{21},κ*N*^{22},κ*N*^{23},κ*N*^{24}}zinc(II) (3):[26,41] A round-bottomed flask (50 mL) equipped with a magnetic stirrer and a septum, was charged with **18** (300 mg, 0.24 mmol) and THF (30 mL). *n*Bu_4NF (1 M in THF; 2.4 mL, 0.48 mmol) was added dropwise. The mixture was stirred for 1 h at 25 °C (after which time TLC showed complete conversion), and then it was poured into a mixture of EtOAc and satd. aq. NH_4Cl (2:1; 80 mL). The phases were separated, and the aqueous phase was extracted with EtOAc (3× 80 mL). The combined organic phases were dried (Na_2SO_4) and filtered, and the solvents were evaporated. Flash chromatography in the dark (SiO_2; *n*-pentane/CH_2Cl_2, 2:1→CH_2Cl_2, 1% v/v Et_3N) gave **3** (155 mg, 68%) as a purple solid. R_f = 0.50 (SiO_2; *n*-pentane/CH_2Cl_2, 2:1), m.p. > 300 °C. ^{1}H NMR (400 MHz, $CDCl_3$): δ = 1.54 (s, 36 H, *t*Bu), 3.31 (s, 2 H, 7-H), 7.82 (t, *J* = 2.0 Hz, 2 H, 4-H), 7.89 (d, *J* = 8.0 Hz, 4 H, 6-H), 8.10 (d, *J* = 2.0 Hz, 4 H, 3-H), 8.21 (d, *J* = 8.0 Hz, 4 H, 5-H), 8.94 (d, *J* = 4.8 Hz, 4 H, 1-H), 9.03 (d, *J* = 4.8 Hz, 4 H, 2-H) ppm. ^{13}C NMR (100 MHz, $CDCl_3$): δ = 31.91, 35.21, 78.22, 83.96, 120.14, 121.06, 121.48, 122.99, 129.91, 130.51, 131.76, 132.73, 134.41, 141.75, 143.78, 148.79, 149.91, 150.74 ppm. IR (neat): $\tilde{\nu}$ = 3268 (m), 3050 (w), 2952 (m), 2924 (m), 2904 (m), 2860 (m), 2105 (w), 1800 (w), 1590 (m), 1523 (w), 1494 (m), 1473 (m), 1463 (w), 1425 (w), 1391 (w), 1361 (m), 1336 (m), 1289 (w), 1261 (m), 1246 (m), 1219 (w), 1204 (m), 1178 (w), 1105 (w), 1070 (m), 1053 (w), 1022 (w), 998 (s), 958 (w), 931 (m), 899 (w), 888 (w), 875 (w), 857 (m), 816 (s), 793 (s), 711 (s), 699 (m), 678 (m), 656 (w), 638 (m), 626 (m) cm^{-1}. UV/Vis ($CHCl_3$): λ_{max} (ε, $M^{-1}cm^{-1}$) = 422 (510800), 549 (36400), 587 (21600) nm. HRMS (MALDI, DCTB): *m*/*z* (%) = 953.4095 (27), 951.4102 (49), 950.4067 (52), 949.4139 (71), 948.4102 (100); calcd. for $C_{64}H_{60}N_4{}^{64}Zn$ $[M]^+$ 948.4104.

{5,15-Bis[3,5-di(*tert*-butyl)phenyl]-10-(4-ethynylphenyl)-20-phenylporphyrinato(2–)-κ*N*^{21},κ*N*^{22},κ*N*^{23},κ*N*^{24}}zinc(II) (4): A round-bottomed flask (50 mL) equipped with a magnetic stirrer and a septum, was charged with **19** (124 mg, 0.12 mmol) and THF (15 mL). *n*Bu_4NF (1 M in THF; 580 μL, 0.12 mmol) was added dropwise. The mixture was stirred for 1 h at 25 °C (after which time TLC showed complete conversion), and then it was poured into a mixture of EtOAc and satd. aq. NH_4Cl (2:1; 50 mL). The phases were separated, and the aqueous phase was extracted with EtOAc (3× 50 mL). The combined organic phases were dried (Na_2SO_4) and filtered, and the solvents were evaporated. Flash chromatography in the dark (SiO_2; *n*-pentane/CH_2Cl_2, 2:1, 1% v/v Et_3N) gave **4** (87 mg, 79%) as a purple solid. R_f = 0.59 (SiO_2; *n*-pentane/CH_2Cl_2, 2:1), m.p. > 300 °C. ^{1}H NMR (400 MHz, $CDCl_3$): δ = 1.55 (s, 36 H, *t*Bu), 3.31 (s, 1 H, 9-H), 7.76 (m, 3 H, 11-H and 12-H), 7.82 (br. s, 2 H, 6-H), 7.90 (d, *J* = 8.0 Hz, 2 H, 8-H), 8.11 (br. s, 4 H, 5-H), 8.22 (d, *J* = 8.8 Hz, 2 H, 7-H), 8.24 (br. d, *J* = 8.0 Hz, 2 H, 10-H), 8.95 (d, *J* = 4.8 Hz, 2 H, 1-H), 8.97 (d, *J* = 4.8 Hz, 2 H, 4-H), 9.02 (d, *J* = 4.8 Hz, 2 H, 3-H), 9.04 (d, *J* = 4.8 Hz, 2 H, 2-H) ppm. ^{13}C NMR (100 MHz, $CDCl_3$): δ = 31.92, 35.22, 78.18, 83.99, 119.89, 121.01, 121.35, 121.44, 122.86, 126.68, 127.64, 129.94, 130.50, 131.64, 132.10, 132.51, 132.66, 134.43, 134.48, 141.85, 143.05, 143.88, 148.76, 149.87, 150.34, 150.65, 150.75 ppm. IR (neat): $\tilde{\nu}$ = 3319 (w), 3058 (w), 2962 (s), 2864 (m), 2108 (w), 1801 (w), 1590 (s), 1523 (w), 1490 (w), 1476 (m), 1463 (w), 1443 (w), 1391 (w), 1361 (m), 1337 (m), 1288 (w), 1261 (w), 1246 (m), 1204 (m), 1178 (w), 1051 (w), 1000 (s), 932 (m), 899 (m), 887 (m), 875 (m), 860 (m), 817 (s), 793 (s), 757 (s), 745 (m), 736 (m), 712 (s), 677 (w), 660 (m), 635 (s) cm^{-1}. UV/Vis ($CHCl_3$): λ_{max} (ε, $M^{-1}cm^{-1}$) = 421 (383400), 548 (26800), 586 (15500) nm. HRMS (MALDI, DCTB): *m*/*z* (%) = 930.4134 (9), 928.4051 (32), 927.4103 (43), 926.4064 (51), 924.4102 (100); calcd. for $C_{62}H_{60}N_4{}^{64}Zn$ $[M]^+$ 924.4104.

[5,15-Bis[3,5-di(*tert*-butyl)phenyl]-10-(4-{2-[4-(dimethylamino)-phenyl]ethynyl}phenyl)-20-(4-ethynylphenyl)porphyrinato(2–)-κ*N*^{21},κ*N*^{22},κ*N*^{23},κ*N*^{24}]zinc(II) (5): A round-bottomed flask (100 mL) was evacuated and purged with N_2 (3×). Porphyrin **3** (100 mg, 0.10 mmol), [$Pd_2(dba)_2$] (14 mg, 0.015 mmol), P(*o*-Tol)$_3$ (37 mg, 0.12 mmol), and 4-bromo-*N*,*N*-dimethylaniline (21 mg, 0.10 mmol) were added. The flask was carefully evacuated and purged with N_2 (3×). Toluene (33 mL) and dry Et_3N (7 mL) were added. The mixture was degassed by three freeze–pump–thaw cycles and put under N_2. It was warmed to 25 °C, heated to 40 °C for 16 h, and cooled to 25 °C. SiO_2 (ca. 5 g) was added, and the solvents were evaporated. Flash chromatography in the dark (SiO_2; *n*-pentane→CH_2Cl_2, 1% v/v Et_3N), followed by GPC (2× Jaigel-2H and Jaigel-2.5 H, $CHCl_3$), gave **5** (12 mg, 11%) as a purple solid. R_f = 0.80 (SiO_2; *n*-pentane/CH_2Cl_2, 1:1), m.p. > 300 °C (decomp.). ^{1}H NMR (600 MHz, $CDCl_3$): δ = 1.54 (s, 36 H, *t*Bu), 2.96 (s, 6 H, Me), 3.31 (s, 1 H, 13-H), 6.68 (d, *J* = 9.0 Hz, 2 H, 10-H), 7.54 (d, *J* = 9.0 Hz, 2 H, 9-H), 7.81 (t, *J* = 1.8 Hz, 2 H, 6-H), 7.89 (d, *J* = 8.4 Hz, 4 H, 8-H), 8.09 (d, *J* = 1.8 Hz, 4 H, 5-H), 8.20 (d, *J* = 8.4 Hz, 2 H, 7-H or 11-H), 8.21 (d, *J* = 8.4 Hz, 2 H, 7-H or 11-H), 8.92 (d, *J* = 4.8 Hz, 2 H, 1-H), 8.98 (d, *J* = 4.8 Hz, 2 H, 2-H), 9.01 (d, *J* = 3.0 Hz, 2 H, 3-H or 4-H), 9.02 (d, *J* = 3.0 Hz, 2 H, 3-H or 4-H) ppm. ^{13}C NMR (150 MHz, $CDCl_3$): δ = 31.91, 35.21, 40.40, 78.17, 83.99, 87.65, 91.83, 110.33, 112.11, 119.96, 120.71, 121.03, 121.42, 122.89, 123.50, 129.63, 129.88, 130.49, 131.65, 131.92, 132.66, 132.98, 134.42, 134.48, 141.82, 142.32, 143.86, 148.75, 149.85, 150.11, 150.33, 150.66, 150.72 ppm. IR (neat): $\tilde{\nu}$ = 3297 (w), 2951 (s), 2923 (s), 2854 (m), 2616 (w), 2494 (w), 2211 (w), 1809 (w), 1741 (w), 1696 (w), 1611 (w), 1591 (m), 1516 (m), 1491 (w), 1474 (m), 1461 (m), 1451 (m), 1425 (w), 1391 (w), 1361 (m), 1337 (m), 1287 (m), 1247 (m), 1216 (m), 1204 (m), 1178 (w), 1154 (w), 1133 (m), 1101 (w), 1069 (m), 1051 (w), 1036 (w), 1022 (w), 997 (s), 928 (m), 901 (m), 885 (w), 875 (w), 860 (m), 822 (s), 809 (s), 796 (s), 752 (s), 733 (s), 715 (s), 666 (m), 650 (m), 621 (m) cm^{-1}. UV/Vis ($CHCl_3$): λ_{max} (ε, $M^{-1}cm^{-1}$) = 423 (175100), 549 (13000), 589 (7500) nm. HRMS (MALDI, DCTB): *m*/*z* (%) = 1073.4860 (11), 1071.4790 (37), 1070.4828 (50), 1069.4785 (50), 1067.4836 (100); calcd. for $C_{72}H_{69}N_5{}^{64}Zn$ $[M]^+$ 1067.4839.

{5,15-Bis[3,5-di(*tert*-butyl)phenyl]-10,20-diphenylporphyrinato(2–)-κ*N*^{21},κ*N*^{22},κ*N*^{23},κ*N*^{24}}zinc(II) (6): A round-bottomed flask (50 mL) was evacuated and purged with N_2 (3×). Porphyrin **7** (195 mg, 0.2 mmol), [$Pd(PPh_3)_4$] (23 mg, 0.02 mmol), and Cs_2CO_3 (828 mg, 2.54 mmol) were added. The flask was carefully evacuated and purged with N_2 (3×). Iodobenzene (245 μL, 2.19 mmol), toluene (20 mL), and H_2O (200 μL) were added. The mixture was degassed by three freeze–pump–thaw cycles and put under N_2. It was warmed up to 25 °C, heated to 100 °C for 20 h, and cooled to 25 °C. SiO_2 (ca. 10 g) was added, and the solvents were evaporated. Flash chromatography in the dark (SiO_2; *n*-hexane→*n*-hexane/CH_2Cl_2, 2:1, 1% v/v Et_3N), followed by GPC (2× Jaigel-2*H* and Jaigel-2.5 H, $CHCl_3$), gave **6** (154 mg, 88%) as a purple solid. R_f = 0.68 (SiO_2; *n*-pentane/CH_2Cl_2, 2:1), m.p. > 300 °C. ^{1}H NMR (400 MHz, $CDCl_3$): δ = 1.53 (s, 36 H, *t*Bu), 7.71–7.77 (m, 6 H, 6-H and 7-H), 7.80 (t, *J* = 1.8 Hz, 2 H, 4-H), 8.10 (d, *J* = 2.0 Hz, 4 H, 3-H), 8.23 [dd, *J* = 2.0, 7.6 Hz, 4 H, 5-H), 8.94 (d, *J* = 4.8 Hz, 4 H, 1-H or 2-H), 8.99 (d, *J* = 4.8 Hz, 4 H, 1-H or 2-H) ppm. ^{13}C NMR (100 MHz, $CDCl_3$): δ = 31.90, 35.20, 120.87, 120.98, 122.61, 126.61, 127.53, 129.96, 131.90, 132.37, 134.49, 142.00, 143.22,

148.65, 150.23, 150.60 ppm. IR (neat): $\tilde{\nu}$ = 2958 (m), 2924 (m), 2859 (m), 1811 (w), 1590 (m), 1524 (w), 1488 (m), 1474 (m), 1461 (m), 1441 (m), 1425 (m), 1392 (m), 1361 (m), 1338 (m), 1287 (m), 1259 (m), 1246 (m), 1217 (m), 1206 (m), 1174 (m), 1158 (m), 1069 (m), 1001 (s), 972 (m), 933 (m), 917 (m), 898 (m), 885 (m), 875 (m), 824 (m), 798 (s), 754 (s), 729 (m), 715 (s), 701 (s), 665 (m), 622 (m) cm^{-1}. UV/Vis ($CHCl_3$): λ_{max} (ε, $M^{-1}cm^{-1}$) = 421 (686900), 548 (25600), 587 (5200) nm. HRMS (MALDI, DCTB): *m*/*z* (%) = 906.4130 (6), 905.4091 (22), 904.4048 (32), 903.4102 (41), 902.4065 (54), 901.4138 (64), 900.4102 (100); calcd. for $C_{60}H_{60}N_4{}^{64}Zn$ $[M]^+$ 900.4104.

(5,15-Bis[3,5-di(*tert*-butyl)phenyl]-10,20-bis{4-[(triisopropylsilyl)-ethynyl]phenyl}porphyrinato(2–)-κ*N*^{21},κ*N*^{22},κ*N*^{23},κ*N*^{24})zinc(II) (18) and (5,15-Bis[3,5-di(*tert*-butyl)phenyl]-10-{4-[(triisopropylsilyl)-ethynyl]phenyl}-20-phenylporphyrinato(2–)-κ*N*^{21},κ*N*^{22},κ*N*^{23},κ*N*^{24})-zinc(II) (19): A round-bottomed flask (100 mL) was evacuated and purged with N_2 (3×). Porphyrin **7** (500 mg, 0.50 mmol), $[Pd(PPh_3)_4]$ (58 mg, 0.05 mmol), and Cs_2CO_3 (21 mg, 6.50 mmol) were added. The flask was carefully evacuated and purged with N_2 (3×). Subsequently, bromide **17** (0.42 g, 1.25 mmol), toluene (50 mL), and H_2O (500 μL) were added. The mixture was degassed by three freeze–pump–thaw cycles and put under N_2. It was warmed up to 25 °C, heated to 110 °C for 20 h, and cooled to 25 °C. SiO_2 (ca. 10 g) was added, and the solvents were evaporated. Flash chromatography in the dark (2× SiO_2; *n*-pentane→*n*-pentane/CH_2Cl_2, 2:1, 1% v/v Et_3N), followed by GPC (2× Jaigel-2H and Jaigel-2.5 H, $CHCl_3$) gave **18** (435 mg, 69%) and **19** (113 mg, 21%) as purple solids.

Data for porphyrin **18**: R_f = 0.83 (SiO_2; *n*-pentane/CH_2Cl_2, 2:1), m.p. > 300 °C. ^{1}H NMR (400 MHz, $CDCl_3$): δ = 1.27 (s, 42 H, *i*Pr), 1.55 (s, 36 H, *t*Bu), 7.82 (br. s, 2 H, 4-H), 7.89 (d, *J* = 7.6 Hz, 4 H, 6-H), 8.10 (br. s, 4 H, 3-H), 8.19 (d, *J* = 7.6 Hz, 4 H, 5-H), 8.90 (d, *J* = 4.6 Hz, 4 H, 1-H), 9.01 (d, *J* = 4.6 Hz, 4 H, 2-H) ppm. ^{13}C NMR (100 MHz, $CDCl_3$): δ = 11.63, 18.97, 31.92, 35.22, 91.72, 107.40, 120.30, 120.99, 122.81, 122.88, 129.97, 130.41, 131.76, 132.62, 134.38, 141.87, 143.36, 148.74, 149.95, 150.69 ppm. IR (neat): $\tilde{\nu}$ = 2945 (m), 2863 (m), 2154 (m), 1811 (w), 1698 (w), 1591 (m), 1525 (w), 1491 (m), 1461 (m), 1425 (w), 1392 (w), 1362 (m), 1338 (m), 1288 (w), 1246 (m), 1219 (m), 1205 (m), 1176 (m), 1101 (w), 1071 (m), 998 (s), 952 (w), 929 (m), 903 (w), 883 (m), 859 (m), 825 (s), 808 (s), 798 (s), 767 (w), 733 (m), 719 (m), 674 (s), 644 (m), 618 (m) cm^{-1}. UV/Vis ($CHCl_3$): λ_{max} (ε, $M^{-1}cm^{-1}$) = 423 (518700), 549 (20600), 588 (5600) nm. HRMS (MALDI, DCTB): *m*/*z* (%) = 1262.6778 (71), 1261.6821 (89), 1260.6796 (100); calcd. for $C_{82}H_{100}N_4Si_2{}^{64}Zn$ $[M]^+$ 1260.6773.

Data for porphyrin **19**: R_f = 0.78 (SiO_2; *n*-pentane/CH_2Cl_2, 2:1), m.p. > 300 °C. ^{1}H NMR (600 MHz, $CDCl_3$): δ = 1.26 (s, 21 H, *i*Pr), 1.54 (s, 36 H, *t*Bu), 7.75 (m, 3 H, 10-H and 11-H), 7.81 (t, *J* = 1.8 Hz, 2 H, 6-H), 7.88 (d, *J* = 8.4 Hz, 2 H, 8-H), 8.10 (d, *J* = 1.8 Hz, 4 H, 5-H), 8.19 (d, *J* = 7.8 Hz, 2 H, 7-H), 8.23 (br. d, *J* = 6.6 Hz, 2 H, 9-H), 8.94 (d, *J* = 4.8 Hz, 2 H, 1-H, 2-H, 3-H or 4-H), 8.95 (d, *J* = 4.8 Hz, 2 H, 1-H, 2-H, 3-H or 4-H), 9.00 (d, *J* = 4.8 Hz, 2 H, 1-H, 2-H, 3-H or 4-H), 9.01 (d, *J* = 4.6 Hz, 2 H, 1-H, 2-H, 3-H or 4-H) ppm. ^{13}C NMR (150 MHz, $CDCl_3$): δ = 11.62, 18.96, 31.90, 35.21, 91.70, 107.40, 120.13, 120.95, 121.24, 122.79, 126.65, 127.60, 129.95, 130.41, 131.70, 132.03, 132.46, 132.58, 134.36, 134.48, 141.88, 143.09, 143.36, 148.72, 149.92, 150.28, 150.61, 150.70 ppm. IR (neat): $\tilde{\nu}$ = 2957 (s), 2922 (s), 2853 (s), 2155 (w), 1710 (w), 1592 (m), 1524 (w), 1484 (w), 1462 (m), 1393 (w), 1378 (w), 1363 (m), 1337 (w), 1287 (w), 1260 (m), 1247 (w), 1219 (w), 1198 (m), 1186 (w), 1203 (w), 1099 (w), 1071 (m), 996 (s), 928 (m), 899 (w), 883 (m), 856 (w), 822 (m), 795 (s), 733 (w), 717 (m), 668 (s) cm^{-1}. UV/Vis ($CHCl_3$): λ_{max} (ε, $M^{-1}cm^{-1}$) = 422 (1389000), 549 (52000), 587 (52100) nm. HRMS (MALDI, DCTB): *m*/*z* (%) = 1084.5422 (44), 1083.5444 (56), 1082.5404 (67), 1080.5446 (100); calcd. for $C_{71}H_{80}N_4Si^{64}Zn$ $[M]^+$ 1080.5438.

CCDC-982227 (for **1**·2THF), -982228 (for **2**·MeOH), -982229 (for **4**·MeOH), -982230 (for **6**) and -982231 (for **19**·MeOH) contain the crystallographic data for this paper and can be obtained free of charge from the Cambridge Crystallographic Data Centre via www.ccdc.cam.ac.uk/data_request/cif.

Supporting Information (see footnote on the first page of this article): General considerations, methods, and materials; synthesis and characterization of compounds **7**, **8**, **14**, and **16**; [2+2] cycloaddition–retroelectrocyclization (CA–RE) reaction of **2** with bis(dicyanovinyl) arene **15**; concentration-dependent ^{1}H NMR spectroscopy studies. DFT-optimized structures of 4-(dimethylamino)-tolane, **2**, and **6**; TGA analysis of **1**–**4** and **6**; copies of UV/Vis spectra, and 1D or 2D NMR spectra of all new compounds.

Acknowledgments

This work was supported by the Swiss National Science Foundation (SNF) (grant number 206021-113149). The research of M. N. A. was carried out within the framework of the action "Supporting Postdoctoral Researchers" of the operational program "Education and Lifelong Learning" (action's beneficiary: General Secretariat for Research and Technology), and was co-financed by the European Social Fund (ESF) and the Greek State. S. N. and T. A. J. acknowledge the SNF (grant numbers 200020-137917, 200020-149713, and 206021-121461). J. N. and T. A. J. gratefully acknowledge the PhD School of the Swiss Nanoscience Institute (SNI) and the SNF in addition to funding from the hosting institutions. The authors thank Dr. Christain Wäckerlin, Dr. Susanne Martens, Dr. Toni Ivas, Mr. Haraldur Gardarsson, Dr. Pablo Rivera Fuentes, Mr. Oliver Dumele, Dr. Nils Trapp, and Dr. Ori Gidron for fruitful discussions. Mr. Marco Martina and Mr. Rolf Schelldorfer are acknowledged for technical support during UHV studies. The authors are also grateful to Mr. Boris Tchitchanov for providing compound **15**, and to Mr. Thomas Schweizer for performing the TGA measurements.

[1] a) T. F. A. De Greef, M. M. J. Smulders, M. Wolffs, A. P. H. J. Schenning, R. P. Sijbesma, E. W. Meijer, *Chem. Rev.* **2009**, *109*, 5687–5754; b) C. A. E. Hauser, S. Zhang, *Chem. Soc. Rev.* **2010**, *39*, 2780–2790; c) J. W. Steed, *Chem. Commun.* **2011**, *47*, 1379–1383; d) L. Maggini, D. Bonifazi, *Chem. Soc. Rev.* **2012**, *41*, 211–241; e) T. R. Cook, Y.-R. Zheng, P. J. Stang, *Chem. Rev.* **2013**, *113*, 734–777; f) A. Das, S. Ghosh, *Angew. Chem. Int. Ed.* **2014**, *53*, 2038–2054; *Angew. Chem.* **2014**, *126*, 2068–2084.

[2] For selected reviews of on-surface supramolecular architectures, see: a) J. V. Barth, G. Costantini, K. Kern, *Nature* **2005**, *437*, 671–679; b) J. V. Barth, *Annu. Rev. Phys. Chem.* **2007**, *58*, 375–407; c) D. Bonifazi, O. Enger, F. Diederich, *Chem. Soc. Rev.* **2007**, *36*, 390–414; d) N. Miyashita, D. G. Kurth, *J. Mater. Chem.* **2008**, *18*, 2636–2649; e) T. Kudernac, S. Lei, J. A. A. W. Elemans, S. De Feyter, *Chem. Soc. Rev.* **2009**, *38*, 402–421; f) D. Bonifazi, S. Mohnani, A. Llanes-Pallas, *Chem. Eur. J.* **2009**, *15*, 7004–7025; g) R. Otero, J. M. Gallego, A. L. V. de Parga, N. Martín, R. Miranda, *Adv. Mater.* **2011**, *23*, 5148–5176.

[3] a) S. R. Forrest, *Nature* **2004**, *428*, 911–918; b) A. P. H. J. Schenning, E. W. Meijer, *Chem. Commun.* **2005**, 3245–3258; c) A. R. Murphy, J. M. J. Fréchet, *Chem. Rev.* **2007**, *107*, 1066–1096.

[4] a) D. L. Taylor, E. S. Woo, K. A. Giuliano, *Curr. Opin. Biotechnol.* **2001**, *12*, 75–81; b) M. Sarikaya, C. Tamerler, A. K.-Y. Jen, K. Schulten, F. Baneyx, *Nat. Mater.* **2003**, *2*, 577–585.

[5] a) J. Otsuki, *Coord. Chem. Rev.* **2010**, *254*, 2311–2341; b) S. Mohnani, D. Bonifazi, *Coord. Chem. Rev.* **2010**, *254*, 2342–2362; c) N. Veling, J. A. A. W. Elemans, R. J. M. Nolte, A. E. Rowan, in: *Handbook of Porphyrin Science with Applications to Chemistry, Physics, Materials Science Engineering, Biology and Medicine* (Eds.: K. M. Kadish, K. M. Smith, R. Guilard), World Scientific Publishing, New Jersey, **2012**, vol. 18, p. 1–56.

[6] For selected studies, see: a) T. Yokoyama, S. Yokoyama, T. Kamikado, Y. Okuno, S. Mashiko, *Nature* **2001**, *413*, 619–621; b) D. Bonifazi, A. Kiebele, M. Stöhr, F. Cheng, T. Jung, F. Diederich, H. Spillmann, *Adv. Funct. Mater.* **2007**, *17*, 1051–1062; c) N. Wintjes, D. Bonifazi, F. Cheng, A. Kiebele, M. Stöhr, T. Jung, H. Spillmann, F. Diederich, *Angew. Chem. Int. Ed.* **2007**, *46*, 4089–4092; *Angew. Chem.* **2007**, *119*, 4167–4170; d) D. Écija, M. Trelka, C. Urban, P. de Mendoza, E. Mateo-Martí, C. Rogero, J. A. Martín-Gago, A. M. Echavarren, R. Otero, J. M. Gallego, R. Miranda, *J. Phys. Chem. C* **2008**, *112*, 8988–8994; e) Z. Shi, N. Lin, *ChemPhysChem* **2010**, *11*, 97–100.

[7] a) L. Grill, M. Dyer, L. Lafferentz, M. Persson, M. V. Peters, S. Hecht, *Nat. Nanotechnol.* **2007**, *2*, 687–691; b) L. Lafferentz, V. Eberhardt, C. Dri, C. Africh, G. Comelli, F. Esch, S. Hecht, L. Grill, *Nat. Chem.* **2012**, *4*, 215–220; c) T. Lin, X. S. Shang, J. Adisoejoso, P. N. Liu, N. Lin, *J. Am. Chem. Soc.* **2013**, *135*, 3576–3582.

[8] a) N. Wintjes, J. Lobo-Checa, J. Hornung, T. Samuely, F. Diederich, T. A. Jung, *J. Am. Chem. Soc.* **2010**, *132*, 7306–7311; b) T. Samuely, S.-X. Liu, N. Wintjes, M. Haas, S. Decurtins, T. A. Jung, M. Stöhr, *J. Phys. Chem. C* **2008**, *112*, 6139–6144.

[9] C. Iacovita, P. Fesser, S. Vijayaraghavan, M. Enache, M. Stöhr, F. Diederich, T. A. Jung, *Chem. Eur. J.* **2012**, *18*, 14610–14613.

[10] The DMAT substituent has also been successfully used for an on-surface click reaction: P. Fesser, C. Iacovita, C. Wäckerlin, S. Vijayaraghavan, N. Ballav, K. Howes, J.-P. Gisselbrecht, M. Crobu, C. Boudon, M. Stöhr, T. A. Jung, F. Diederich, *Chem. Eur. J.* **2011**, *17*, 5246–5250.

[11] M. J. Frisch et al., *Gaussian 09*, revision A.1, Gaussian, Inc., Wallingford CT, **2009**; see the Supporting Information for the full list of the coauthors.

[12] N. Wintjes, J. Hornung, J. Lobo-Checa, T. Voigt, T. Samuely, C. Thilgen, M. Stöhr, F. Diederich, T. A. Jung, *Chem. Eur. J.* **2008**, *14*, 5794–5802.

[13] B. J. Littler, Y. Ciringh, J. S. Lindsey, *J. Org. Chem.* **1999**, *64*, 2864–2872 and references cited therein.

[14] a) D. S. Sharada, A. Z. Muresan, K. Muthukumaran, J. S. Lindsey, *J. Org. Chem.* **2005**, *70*, 3500–3510; b) D. K. Dogutan, M. Ptaszek, J. S. Lindsey, *J. Org. Chem.* **2008**, *73*, 6187–6201; c) D. K. Dogutan, J. S. Lindsey, *J. Org. Chem.* **2008**, *73*, 6728–6742.

[15] For selected examples, see: a) A. G. Hyslop, M. A. Kellett, P. M. Iovine, M. J. Therien, *J. Am. Chem. Soc.* **1998**, *120*, 12676–12677; b) P. Weyermann, J.-P. Gisselbrecht, C. Boudon, F. Diederich, M. Gross, *Angew. Chem. Int. Ed.* **1999**, *38*, 3215–3219; *Angew. Chem.* **1999**, *111*, 3400–3405; c) D. Bonifazi, G. Accorsi, N. Armaroli, F. Song, A. Palkar, L. Echegoyen, M. Scholl, P. Seiler, B. Jaun, F. Diederich, *Helv. Chim. Acta* **2005**, *88*, 1839–1884; d) F. Cheng, S. Zhang, A. Adronov, L. Echegoyen, F. Diederich, *Chem. Eur. J.* **2006**, *12*, 6062–6070.

[16] L.-A. Fendt, M. Stöhr, N. Wintjes, M. Enache, T. A. Jung, F. Diederich, *Chem. Eur. J.* **2009**, *15*, 11139–11150 and references cited therein.

[17] It is worth mentioning that the separation of porphyrins **1** and **2** by GPC was very difficult, probably due to intense aggregation. Successful GPC analysis was carried out using 5–10 mg of mixture per injection.

[18] F. E. Goodson, T. I. Wallow, B. M. Novak, *J. Am. Chem. Soc.* **1997**, *119*, 12441–12453.

[19] For the formation of scrambled products under Sonogashira cross-coupling conditions, see: a) R. W. Wagner, Y. Ciringh, C. Clausen, J. S. Lindsey, *Chem. Mater.* **1999**, *11*, 2974–2983; b) M. Kozaki, S. Morita, S. Suzuki, K. Okada, *J. Org. Chem.* **2012**, *77*, 9447–9457.

[20] T. E. Barder, S. D. Walker, J. R. Martinelli, S. L. Buchwald, *J. Am. Chem. Soc.* **2005**, *127*, 4685–4696.

[21] a) T. Michinobu, J. C. May, J. H. Lim, C. Boudon, J.-P. Gisselbrecht, P. Seiler, M. Gross, I. Biaggio, F. Diederich, *Chem. Commun.* **2005**, 737–739; b) T. Michinobu, C. Boudon, J.-P. Gisselbrecht, P. Seiler, B. Frank, N. N. P. Moonen, M. Gross, F. Diederich, *Chem. Eur. J.* **2006**, *12*, 1889–1905.

[22] This product was unstable under the conditions of chromatographic purification using: (a) neutral Al_2O_3 (Act. III) or acidic SiO_2 in the presence of 1% Et_3N; and (b) GPC on polystyrene–divinylbenzene as a stationary phase. However, compound **14** was successfully purified by precipitation from a CH_2Cl_2 solution upon addition of *n*-hexane.

[23] F. Silvestri, M. Jordan, K. Howes, M. Kivala, P. Rivera-Fuentes, C. Boudon, J.-P. Gisselbrecht, W. B. Schweizer, P. Seiler, M. Chiu, F. Diederich, *Chem. Eur. J.* **2011**, *17*, 6088–6097.

[24] a) A. Godt, Ö. Ünsal, M. Roos, *J. Org. Chem.* **2000**, *65*, 2837–2842; b) B. Felber, F. Diederich, *Helv. Chim. Acta* **2005**, *88*, 120–153; c) F. Himmelsbach, M. Eckhardt, P. Eickelmann, L. Thomas, E. L. Barsoumian, US 2006 0189548 A1, **2006**.

[25] a) H. Dube, B. Kasumaj, C. Calle, M. Saito, G. Jeschke, F. Diederich, *Angew. Chem. Int. Ed.* **2008**, *47*, 2600–2603; *Angew. Chem.* **2008**, *120*, 2638–2642; b) H. Dube, B. Kasumaj, C. Calle, B. Felber, M. Saito, G. Jeschke, F. Diederich, *Chem. Eur. J.* **2009**, *15*, 125–135.

[26] D. Heim, K. Seufert, W. Auwärter, C. Aurisicchio, C. Fabbro, D. Bonifazi, J. V. Barth, *Nano Lett.* **2010**, *10*, 122–128.

[27] R. K. Lammi, A. Ambroise, T. Balasubramanian, R. W. Wagner, D. F. Bocian, D. Holten, J. S. Lindsey, *J. Am. Chem. Soc.* **2000**, *122*, 7579–7591.

[28] a) M. P. Byrn, C. J. Curtis, Y. Hsiou, S. I. Khan, P. A. Sawin, S. K. Tendick, A. Terzis, C. E. Strouse, *J. Am. Chem. Soc.* **1993**, *115*, 9480–9497; b) R. K. Kumar, S. Balasubramanian, I. Goldberg, *Inorg. Chem.* **1998**, *37*, 541–552; c) M. Palacio, V. Mansuy-Mouries, G. Loire, K. Le Barch-Ozette, P. Leduc, K. M. Barkigia, J. Fajer, P. Battioni, D. Mansuy, *Chem. Commun.* **2000**, 1907–1908; d) X. Shi, Sk. R. Amin, L. S. Liebeskind, *J. Org. Chem.* **2000**, *65*, 1650–1664; e) B. M. J. M. Suijkerbuijk, D. M. Tooke, A. L. Spek, G. van Koten, R. J. M. Klein Gebbink, *Chem. Asian J.* **2007**, *2*, 889–903.

[29] For axial ligation of THF to zinc(II) porphyrin, see: a) C. K. Schauer, O. P. Anderson, S. S. Eaton, G. R. Eaton, *Inorg. Chem.* **1985**, *24*, 4082–4086; b) S. M. LeCours, S. G. DiMagno, M. J. Therien, *J. Am. Chem. Soc.* **1996**, *118*, 11854–11864; c) K. Kobayashi, M. Koyanagi, K. Endo, H. Masuda, Y. Aoyama, *Chem. Eur. J.* **1998**, *4*, 417–424; d) N. Ehlinger, W. R. Scheidt, *Inorg. Chem.* **1999**, *38*, 1316–1321; e) A. Zingg, B. Felber, V. Gramlich, L. Fu, J. P. Collman, F. Diederich, *Helv. Chim. Acta* **2002**, *85*, 333–351.

[30] a) D. Braga, F. Grepioni, E. Tedesco, *Organometallics* **1998**, *17*, 2669–2672; b) G. R. Desiraju, T. Steiner, in: *The Weak Hydrogen Bond in Structural Chemistry and Biology*, Oxford University Press, Oxford, UK, **1999**, p. 29–120; c) T. Steiner, *Angew. Chem. Int. Ed.* **2002**, *41*, 48–76; *Angew. Chem.* **2002**, *114*, 50–80.

[31] a) Y. Umezawa, S. Tsuboyama, K. Honda, J. Uzawa, M. Nishio, *Bull. Chem. Soc. Jpn.* **1998**, *71*, 1207–1213; b) V. B. Medaković, G. A. Bogdanović, M. K. Milčić, G. V. Janjić, S. D. Zarić, *J. Inorg. Biochem.* **2012**, *117*, 157–163; c) B. K. Mishra, S. Karthikeyan, V. Ramanathan, *J. Chem. Theory Comput.* **2012**, *8*, 1935–1942.

[32] F. Bebensee, C. Bombis, S.-R. Vadapoo, J. R. Cramer, F. Besenbacher, K. V. Gothelf, T. R. Linderoth, *J. Am. Chem. Soc.* **2013**, *135*, 2136–2139.

[33] D. Chylarecka, C. Wäckerlin, T. K. Kim, K. Müller, F. Nolting, A. Kleibert, N. Ballav, T. A. Jung, *J. Phys. Chem. Lett.* **2010**, *1*, 1408–1413.
[34] It is worth mentioning that if the decomposition is caused by temperature and not by the substrate, other UHV-compatible thin-film deposition techniques could be used, e.g., the electrospray technique. For selected references regarding the electrospray technique, see: a) A. Jaworek, *J. Mater. Sci.* **2007**, *42*, 266–297; b) S. Rauschenbach, R. Vogelgesang, N. Malinowski, J. W. Gerlach, M. Benyoucef, G. Costantini, Z. Deng, N. Thontasen, K. Kern, *ACS Nano* **2009**, *3*, 2901–2910; c) M. Pauly, M. Sroka, J. Reiss, G. Rinke, A. Albarghash, R. Vogelgesang, H. Hahne, B. Kuster, J. Sesterhenn, K. Kern, S. Rauschenbach, *Analyst* **2014**, *139*, 1856–1867.
[35] A monolayer (ML) is defined as the amount of molecules that entirely cover the substrate.
[36] a) D. Heim, D. Écija, K. Seufert, W. Auwärter, C. Aurisicchio, C. Fabbro, D. Bonifazi, J. V. Barth, *J. Am. Chem. Soc.* **2010**, *132*, 6783–6790; b) D. Écija, K. Seufert, D. Heim, W. Auwärter, C. Aurisicchio, C. Fabbro, D. Bonifazi, J. V. Barth, *ACS Nano* **2010**, *4*, 4936–4942.
[37] a) H.-Y. Gao, H. Wagner, D. Zhong, J.-H. Franke, A. Studer, H. Fuchs, *Angew. Chem. Int. Ed. Engl.* **2013**, *52*, 4024–4028; *Angew. Chem.* **2013**, *125*, 4116–4120. For the on-surface polymerization of 1,4-diethynylbenzene on Cu(111) after annealing, see also: b) J. Eichhorn, W. M. Heckl, M. Lackinger, *Chem. Commun.* **2013**, *49*, 2900–2902.
[38] a) C. Glaser, *Ber. Dtsch. Chem. Ges.* **1869**, *2*, 422–424; b) C. Glaser, *Ann. Chem. Pharm.* **1870**, *154*, 137–171.
[39] a) T. A. Jung, R. R. Schlittler, J. K. Gimzewski, *Nature* **1997**, *386*, 696–698; b) T. Yokoyama, S. Yokoyama, T. Kamikado, S. Mashiko, *J. Chem. Phys.* **2001**, *115*, 3814–3818; c) T. Yokoyama, T. Kamikado, S. Yokoyama, S. Mashiko, *J. Chem. Phys.* **2004**, *121*, 11993–11997.
[40] J. V. Barth, H. Brune, G. Ertl, R. J. Behm, *Phys. Rev. B* **1990**, *42*, 9307–9318.
[41] F. Tancini, F. Monti, K. Howes, A. Belbakra, A. Listorti, W. B. Schweizer, P. Reutenauer, J.-L. Alonso-Gómez, C. Chiorboli, L. M. Urner, J.-P. Gisselbrecht, C. Boudon, N. Armaroli, F. Diederich, *Chem. Eur. J.* **2014**, *20*, 202–216.

Received: May 26, 2014
Published Online: July 30, 2014

